MASTER'S THESIS

Physiologically Based Kinetic (PBK) Model of the Goat

Dekker, S. (Sary)

Award date:
2020

Physiologically Based Kinetic (PBK) Model of the Goat

Thesis MSc Environmental Sciences

Sary Dekker
2020
Vakgroep Milieuwetenschappen
Open Universiteit

Radboud University

Open Universiteit
www.ou.nl

Physiologically Based Kinetic (PBK) Model of the Goat

Fysiologisch Gebaseerd Kinetisch Model van de Geit

Thesis Committee:

First OU Supervisor: Prof. Dr. Ad Ragas - Radboud University, Nijmegen
Second OU Supervisor: Dr. Lily Fredrix - Open Universiteit, Heerlen
External Supervisor: Leonie Lautz, MSc. - Radboud University, Nijmegen

Contents

List of Figures

Abstract

Physiologically Based Kinetic (PBK) models predict the internal concentration of chemicals in different organs after exposure. They are developed and applied to reduce animal studies for risk assessment. Goats are commonly kept for both recreation and consumption, making it a relevant species for assessing the risk of chemical exposures, e.g. due to medicine treatment or environmental pollution. In this study, an existing generic PBK model, previously developed by Radboud University, was adjusted to accurately fit the goat physiology. It was then implemented and validated. The necessary model parameters were obtained by systematic literature review. The adjusted model was implemented into the software program R. In the early exposure phases, the new goat model accurately predicts internal tissue concentrations. This is not the case for all biological processes or in later exposure phases. The main reason for this is the lack of available physiological data for goats, such as body weight of organs and blood flow fractions. For the missing parameters, values for sheep were used. In addition, insufficient suitable studies were available for the validation of the goat-adjusted model. Here, values for toxicokinetic parameters, such as the absorption rate constant and clearance rates, were unavailable. Allometric scaling was used to extrapolate values for these parameters, using data from sheep and cattle. More in vitro and in vivo studies are necessary to reduce the knowledge gaps to allow the reliable application of the generic PBK model for goats.

Samenvatting

Fysiologisch gebaseerde kinetische modellen voorspellen de interne concentraties van (chemische) stoffen in verschillende organen na blootstelling. Ze worden ontwikkeld en toegepast om het benodigde aantal dierproeven voor risicobeoordeling te reduceren. Geiten worden veel gehouden voor zowel recreatieve als consumptiedoeleinden. Dit maakt het een relevante soort voor risicobeoordeling van bijvoorbeeld milieuvervuiling of medicijngebruik. In deze studie wordt een bestaand generiek model (eerder ontwikkeld door de Radboud Universiteit) aangepast om de fysiologie van de geit nauwkeurig te beschrijven. Het model is daarna geïmplementeerd en gevalideerd. De nodige model-
parameters zijn gevonden met behulp van literatuurstudie. Het aangepaste model is geïmplementeerd in de software R. In vroege blootstellingsfases, voorspelt het nieuwe geitmodel de interne concentraties nauwkeurig. Dit is niet het geval voor alle biologische processen en tijdens latere blootstellingsfases. De belangrijkste reden hiervoor is het gebrek aan beschikbare fysiologische data, zoals orgaangewichten en bloedstromen, voor geiten. Voor de missende parameters zijn waardes van het schaap gebruikt. Ook waren onvoldoende geschikte studies beschikbaar voor de validatie van het aangepaste model. In de beschikbare studies misten de waardes voor de benodigde toxicokinetische parameters, zoals de absorptiecoefficient. Voor het verkrijgen van waardes voor deze parameters is allometrisch schaling, met behulp van data van schaap en rundvee, gebruikt. Meer in vitro en in vivo studies zijn nodig om de kennislacunes te verminderen om dit generieke model toepasbaar te maken voor de geit.

Chapter 1

Goal and Problem Description

1.1 Risk Assessment

There are many chemicals in the environment. Some of these chemicals are natural, while others are synthetically made by industries. These chemicals, especially those that are synthetically made, can cause harm to the environment as well as human health. Because the effects of chemicals on human, animal and environmental health are often unclear, risk assessments can be performed to determine this risk.

Due to the risks associated with chemicals, legislation has been developed and is continuously applied by multiple organizations. The European Food Safety Authority (EFSA) is such an organization (EFSA, 2016). Methods for risk assessment have been developed and are harmonized in order to make the process more transparent, results more comparable and communication about the risks possible (WHO, 2009). This must lead to implementable legislation, policy and regulations.

1.2 PBK Models and Risk Assessment

The World Health Organization (WHO) defines Physiologically Based Pharmacokinetic (PBPK) models as "quantitative descriptions of the absorption, distribution, metabolism and excretion (ADME) of chemicals in biota based on interrelationships among key physiological, biochemical and physicochemical determinants of these processes" (WHO, 2010)[1].

PBK models are one-compartmental or multi-compartmental. In a one-compartmental PBK model, the compartment represents a whole organism. For multi-compartmental PBK models, each compartment is based on organs and tissue groups, with physiological characteristics often based on experimental data (Chiu et al., 2007; Clewell & Clewell, 2008). As is visible in Figure 1.1, the PBK model is therefore shown as a scheme of boxes and arrows (WHO, 2010). Each of these represents a realistic organ or group of organs or physical process.

PBK models are important tools for chemical risk assessment (Chiu et al., 2007; Clark et al., 2004; Clewell & Clewell, 2008; WHO, 2010). These models can be used in several ways, which makes them useful for risk assessments involving human health, such as extrapolations across studies, species, exposure routes and dose levels (Barton et al., 2007; Chiu et al., 2007; Clark et al., 2004; Clewell & Clewell, 2008; WHO, 2010). These model applications could lead to less animal testing. Therefore the development and use of PBK models may have a positive influence on animal welfare.

1.3 Problem Statement

In recent years, multiple PBK models have been developed in the field of animal health and veterinary medicine. These were mostly used for predictions of tissue residues and withdrawal intervals in farm animals (Lin et al., 2016). While for other species, such as rats, mice, chicken, cows, sheep and swine, multiple PBK models are available, only one PBK model was found in literature for the goat. This model was specifically developed for tulathromycin (Leavens et al., 2011).

[1]Note: the terms PBK, PBPK, PBTK and PBBK are all synonymous (Paini et al., 2019). I have chosen to use 'Physiologically Based Kinetic (PBK) model' for this thesis, unless otherwise specified, as this is the most accurate term.

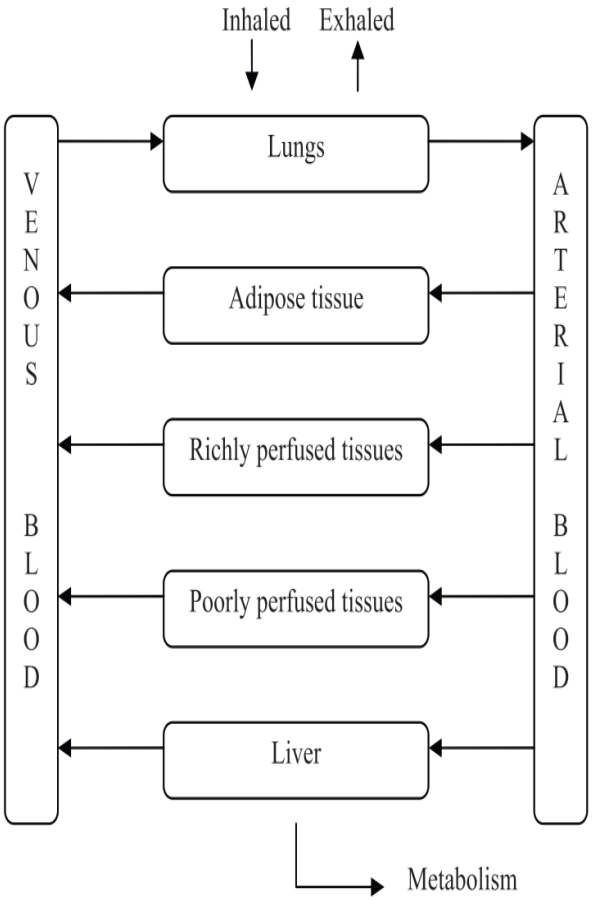

Figure 1.1: An example of a multi-compartmental PBK model (WHO, 2010)

It is inefficient for risk assessors, such as EFSA, to continuously develop new PBK models for different species and each chemical. They prefer a generic PBK model that can be used for different species as well as different chemicals. Therefore, EFSA requested several research institutes to develop generic tools and methods for PBK modeling (Lautz et al., 2017). This led to the development of a generic PBK model structure, which is compatible with chicken, cattle, swine and sheep, by Radboud University Nijmegen, the Netherlands.

Goats are another category of commonly kept farm animals, both for recreation as well as for consumption. In 2016, the EU held 12.8 million goats for milk and meat production (EU, 2018). Goat-related products are thus important consumption products in the EU. This makes it a priority to assess the potential risks of chemicals associated with these products and the welfare of the goats. Therefore, it is desirable to also develop a generic PBK model for this species.

1.4 Research Objective

The aim of this study is to adapt the existing generic Physiologically Based Kinetic (PBK) modeling platform for farm animals developed by Radboud University to accurately describe the internal dose, in blood and/or urine and possibly target organs, of compounds in the goat. The model must be usable for different chemical compounds.

1.5 Research Questions

The research objective has led to the following main question:

Can the available PBK model structure for farm animals as developed by Lautz et al. (2017) be adapted and parameterized to result in a PBK model for goats that can be used to accurately describe the internal dose of compounds in these animals?

The main question can be divided into the following sub-questions:

1. What does the current generic PBK model of Lautz et al. (2017) look like?
2. What compartments must be included in the PBK model to accurately reflect the physiology of the goat?
3. What (physiological) processes must be included in the PBK model to accurately reflect the fate of chemicals in the goat?
4. What information is available on the compartments and (physiological) processes of the goat and how can this information be used to optimally parameterize the goat model?
5. What data is available for the validation of the PBK model?
6. How does the PBK model perform based on this validation data?

1.6 Research Method

First the existing generic PBK model structure will be described. This model has already been implemented into the statistical software suit R. After this description, a literature study will be conducted. The literature study should clarify whether there are differences between goats and other farm animal species that must be taken into consideration for the PBK model. It should supply the information necessary to determine which compartments and (physiological) processes must be implemented in the goat-specific PBK model.

If found necessary, adjustments will be made to the generic PBK model structure by adding the goat-specific compartments and/or (physiological) processes. These changes should make the model suitable for the goat. The necessary physiological parameters will also be adjusted to make the model suitable for the goat. Afterwards, another literature study will be conducted in order to find experimental data which can be used to validate the PBK model for the goat. This data will be specific for certain chemicals, namely ivermectin, chloramphenicol and moxifloxacin. These compounds were chosen because of the availability of data on their tissue distribution after oral or intravenous application.

Next, the found information will be put into the adjusted goat PBK model. After this, the model is run in R. The results produced by the adjusted PBK model will be compared to the experimental data and conclusions will be drawn from these results. Figure 1.2 shows a flowchart summarizing the research approach.

1.7 Reader's guide

Figure 1.2 shows the reader's guide for this thesis. Chapter 2 describes the current generic PBK model, as made by Lautz et al. (2017). It shows the compartments (Section 2.1) and mathematical equations to show relations between the compartments in Section 2.2. In Chapter 3 the current model is adapted to become goat-specific. This is divided in the necessary compartments (Section 3.1) and the general model parameters needed for the goat-adjusted model (Section 3.2). Then the parameters are implemented into the model, which is validated in Chapter 4. Section 4.1 defines the selection process of the validation studies, after which the model is run and Sections 4.2 through 4.4 give specific explanations for the three chosen studies and their results. Chapter 5 discusses the found results, draws conclusions and gives recommendations. The model code is added in Appendix A. The raw results of the model runs for validations are available in Appendix B.

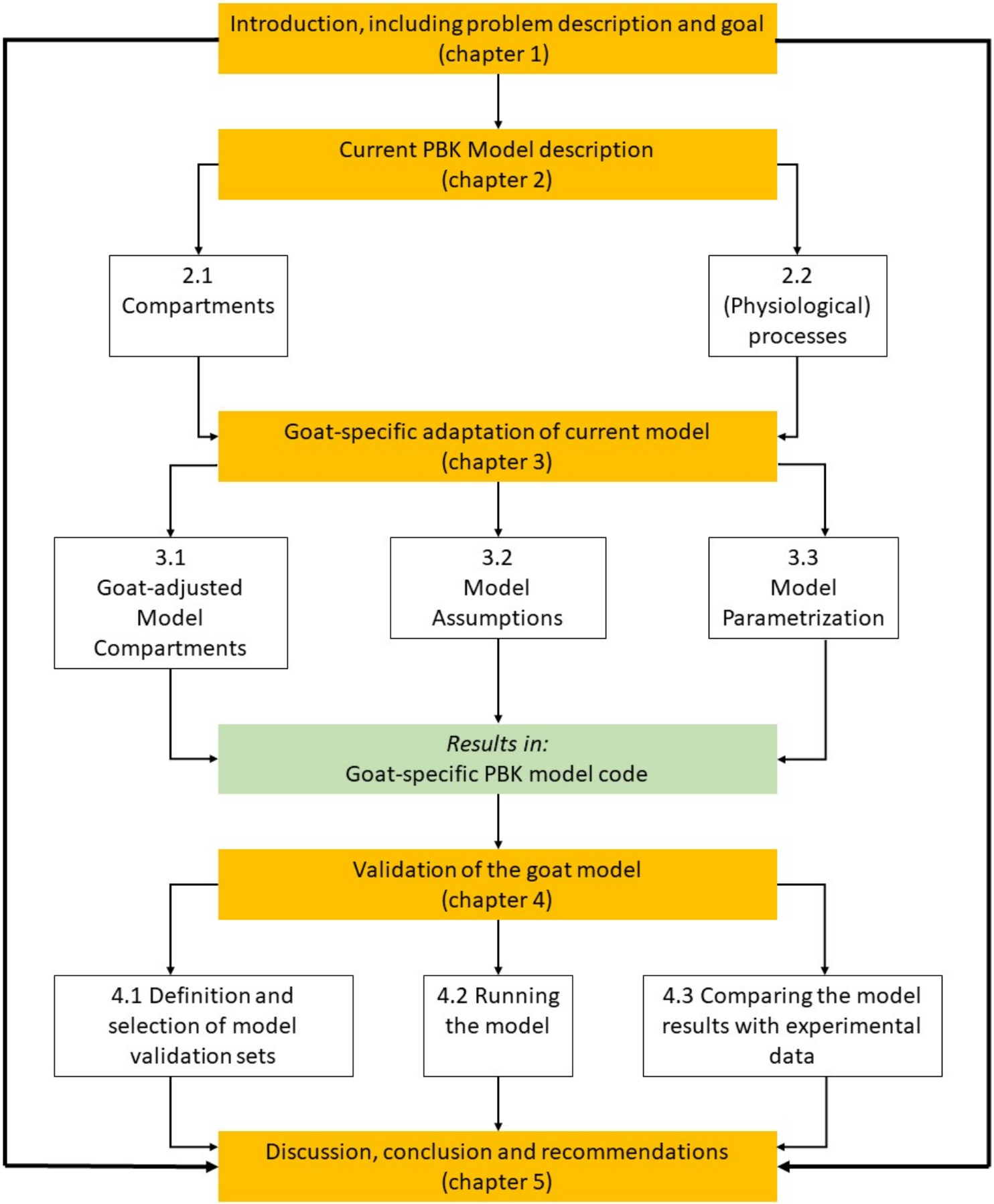

Figure 1.2: Flowchart summarizing the research approach.

Chapter 2

Description of Current PBK Model

The PBK model developed by Lautz et al. (2017) is a generic PBK model that can be used for cattle, sheep, swine and chicken. It consists of multiple compartments that interact with each other through different (physiological) processes. Figure 2.1 shows an example when this PBK model is applied to the swine. This chapter describes the current generic PBK model and supplies the mathematical equations showing the interactions between the different compartments and processes.

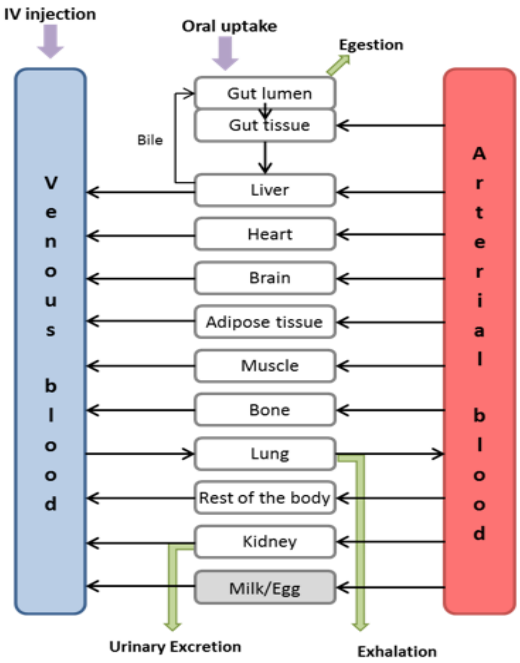

Figure 2.1: Multi-compartmental generic PBK model for the following species: cattle, sheep, swine and chicken (Lautz et al., 2017).

2.1 Compartments

What happens to a substance when it enters the body, depends on the characteristics of the involved species as well as those of the substance. How a PBK model deals with these characteristics depends on whether it is a one-compartmental or multi-compartmental model. The current generic PBK model, as developed by Lautz et al. (2017), is a multi-compartmental PBK model. This means that the body is not seen as a whole, as is the case for a one-compartmental model, but as having multiple compartments, such as heart, liver, lungs and blood.

The body consists of multiple organs, such as the heart, lungs, liver and intestine. Several of these organs are species-specific. For example, ruminant species have multiple organs which together make up the stomach, while for other species the stomach is one organ. Each of the organs is a homogeneous compartment in the multi-compartmental PBK model. Other compartments also play a role in processing chemicals in the body. Blood for example is a compartment that influences the distribution of chemicals

throughout the body. Some chemicals may also be stored in fat or muscle tissue. These compartments are therefore also included in the multi-compartmental PBK model.

The following compartments are present in the current generic PBK model (Lautz et al., 2017) :

- Heart;
- Brain;
- Lung;
- Blood;
- Gizzard;
- Crop;
- Intestine;
- Liver;
- Kidney;
- Stomach;
- Ruminant stomach, consisting of:
  - Rumen;
  - Reticulum;
  - Omasum;
  - Abomasum;
- Reproduction organs (lumped);
- Mammary gland;
- Fat;
- Muscle;
- Lumen; and
- Rest of Body

2.2 (Physiological) Processes

The different compartments interact with each other and the chemical through different (physiological) processes, the so-called ADME processes: Absorption, Distribution,
Metabolism and Excretion. The toxicokinetic data for chemicals going through these processes is key information needed to create a PBK model (EFSA, 2014). The current generic PBK model is therefore also based on the ADME processes. The processes must be translated into mathematical equations to be integrated into the PBK model. Before the mathematical equations will be given, a short explanation is supplied for each of the ADME processes.

Absorption

The first of the processes is absorption. The World Health Organization (WHO) has defined absorption as: 'the process by which a substance is transferred from the site of administration into the circulation. For chemicals in food, absorption usually refers to passage across the gut wall into the circulation, although for some chemicals, uptake may be only as far as the epithelium of the gastrointestinal tract' (WHO, 2010). In the field of food safety, the most common route of exposure to consider is oral ingestion. After ingestion, the compound travels over the intestinal wall into the blood of the portal vein, which transports it into the liver and where it becomes bioavailable when entering the systemic circulation (EFSA, 2014). The fraction of the drug that reaches systemic circulation is called oral bioavailability. Oral bioavailability depends on multiple factors, including solubility, dissolution, permeability, transporter affinity, metabolism in the lumen, intestine and/or liver (Bueters et al., 2013).

Distribution

When a compound is in the systemic circulation, it can be distributed throughout the body to the different compartments (EFSA, 2014). The amount of compound that can be received and can remain in the organ or tissue, differs for each organ or tissue. The distribution of a compound between the blood and the tissue can continue taking place until a steady-state has been found. The distribution rate for compounds depends on the following factors:

- vascular permeability;
- regional blood flow;
- cardiac output;
- perfusion rate of the tissues;
- tissue and plasma protein binding ability; and

- lipophilicity (EFSA, 2014).

Of the above-mentioned factors, the ability of a compound to bind to protein is most important. This is a quality that differs greatly between compounds and determines how much of the compound is free to be distributed into the tissues and organs, and with that influences the toxicokinetics in general (EFSA, 2014). The ability of the compound to bind to proteins therefore determines the tissue:blood partitioning coefficient of the compound (Yoon et al., 2012).

Metabolism

The next ADME process is metabolism. Metabolism is the breakdown of a compound within an organism. The metabolism of chemicals can occur in any tissue of the body (Chiu et al., 2007; EFSA, 2014). The two most important sites of the body where metabolism takes place are the intestinal lumen and the liver. In addition to metabolism by these two compartments, metabolism taking place in the lungs is also included in the current generic PBK model.

Distinction is made between phase I and phase II metabolism. During phase I, a hydrophobic compound is transformed into a polar substance. In phase II, the polar substance is transformed into a hydrophilic substance, the conjugate (Yoon et al., 2012). In general, this conjugate is excreted with the bile. However, it is also possible for the conjugated compound to be de-conjugated.

When enterohepatic circulation takes place, the chemical compound enters the liver, is metabolized and is excreted into the intestinal lumen. Here, bacteria can convert the metabolized compound back into the original parent compound. This newly created parent compound is then again absorbed into the blood of the portal vein and distributed to the liver to be metabolized. Therefore, for some chemicals, part of the compound is recycled, influencing the overall metabolism rate.

Excretion

The last of the ADME processes is excretion. Different organs are involved in the excretion process, such as the kidneys, liver, lungs and skin (EFSA, 2014). In the current model, excretion through the skin has not been taken into consideration. For food safety, excretion through the reproductive system must also be taken into consideration (Lautz et al., 2017). In the current PBK model, routes for livestock include excretion via milk for mammals (cow and sheep) and via eggs for the chicken.

It is complicated to determine the renal excretion, due to the tubular transport structures of the kidney. Besides the difficult structure, there are also multiple transporter proteins involved, complicating the situation further. In the current PBK model, default assumptions are made about the excretion of compounds, but more research into the interaction between transporter proteins and renal excretion might lead to a better understanding of renal clearance as derived from the glomerular filtration rate (EFSA, 2014; Lautz et al., 2017).

In the following sections, the (physiological) processes are described for each of the compartments, as they are implemented in the generic PBK model by Lautz et al. (2017). For each compartment, the necessary ADME processes are described and translated into mathematical equations. There are several general model equations, which are followed by the organ specific equations.

2.2.1 General Model Equations

In general, the change in the amount of a chemical in an organ is determined by the difference between the incoming and outgoing amounts of the compound. This is dependent on the amount of the chemical that is metabolized, accumulated, excreted and transported to the venous blood (Lautz et al., 2017). The arterial blood brings the compound to the organ, while it flows away from the organ with the venous blood. Equation 2.1 describes the change in the amount of chemical over time in a general equation. This general equation is applicable to all organs, except if otherwise specified in Section 2.2.2.

$$\frac{dM_{\text{tissue}}}{dt} = Q_{\text{t}} * (C_{\text{art}} - C_{\text{ven}}) \tag{2.1}$$

where:

$\frac{dM_{\text{tissue}}}{dt}$	=	change in the amount of chemical in a compartment (μmol/h);
Q_{t}	=	blood flow through the tissue (L/h);
C_{art}	=	arterial blood chemical concentration (μmol/L);
C_{ven}	=	venous blood chemical concentration (μmol/L).

Lautz et al. (2017) assume a blood flow-limited model. This means that the concentration of the compound in the tissue is equal to the concentration of the compound in the blood leaving the tissue. Therefore, the concentration of the compound in the venous blood (C_{ven}) can be substituted by the tissue concentration (C_{t}) and the tissue/blood partitioning coefficient (P_{t}), leading to Equation 2.2.

$$\frac{dM_{\text{tissue}}}{dt} = Q_{\text{t}} * (C_{\text{art}} - \frac{C_{\text{t}}}{P_{\text{t}}}) \tag{2.2}$$

where:

C_{t}	=	tissue chemical concentration (μmol/kg);
P_{t}	=	tissue/blood partitioning coefficient (-).

Entry of Compounds into the Body

In the current PBK model, chemicals enter the body either through feed or through intravenous injection (IV). Exposure through inhalation, as well as dermal exposure, is not implemented in this model. The route of exposure determines into which of the compartments (see Section 2.1) the chemical is released and what happens to the chemical after it has entered the body. Equation 2.3 shows the input of the compound via feed. It describes the combination of a bolus regime and a continuous regime for oral uptake.

$$\frac{dM_{\text{feed}}}{dt} = E_{\text{bolus}}[i] * Q_{\text{bolus}} + E_{\text{cont}}[i] * Q_{\text{ingest}} \tag{2.3}$$

where:

$\frac{dM_{\text{feed}}}{dt}$	=	intake rate of the compound through feed (mg/min);
$E_{\text{bolus}}[i]$	=	administered dosage for a bolus regime (mg);
Q_{bolus}	=	exposure duration (min^{-1});
$E_{\text{cont}}[i]$	=	administered dosage for a continuous regime (mg/kg feed);
Q_{ingest}	=	ingestation rate (kg feed/min).

The second route of exposure is via injection. Equation 2.4 shows the mathematical equation describing the input via an IV. Unlike the input via food, the input via injection is always following a bolus regime. Therefore, there is no term describing a continuous regime in this equation.

$$\frac{dM_{\text{iv}}}{dt} = E_{\text{iv}}[i] * Q_{\text{iv}} \tag{2.4}$$

where:

$\frac{dM_{\text{iv}}}{dt}$	=	intake rate of the compound administered through an IV (mg/h);
$E_{\text{iv}}[i]$	=	exposure dose administered (mg);
Q_{iv}	=	amount of times administered (h^{-1}).

2.2.2 Compartment Specific Equations

In this section, the mathematical equations are given for each specific compartment. For each of the compartments, the role of the ADME processes is described.

Arterial Blood

The first compartment is the arterial blood. The arterial blood flows away from the heart and is therefore important in the distribution of compounds. The concentration of the compound in the arterial blood (C_{art}) is calculated by dividing the mass of the compound in the arterial blood (M_{art}) by the volume of the arterial blood (V_{art}), as is shown in Equation 2.5. The assumption is made that there is no difference between the concentration of the compound in the arterial blood leaving the heart and the arterial blood entering the organs.

$$C_{\text{art}} = \frac{M_{\text{art}}}{V_{\text{art}}} \tag{2.5}$$

where:

C_{art}	=	concentration of compound in arterial blood entering the organs (μmol/L);
M_{art}	=	mass of the compound in the arterial blood (μmol);
V_{art}	=	volume of the arterial blood.

Venous Blood

Another important compartment for distribution is the venous blood. The venous blood flows from the organs to the heart. The model assumes that all venous blood, which leaves the tissues and/or organs, is mixed. Equation 2.6 takes this assumption into consideration and shows the total mass of the compound leaving the organs and flowing into the venous blood.

$$M_{\text{ven}} = \sum_{T}^{notliver+gut} Q_{\text{t}} * (\frac{C_{\text{t}}}{P_{\text{t}}}) + (Q_{\text{gut}} + Q_{\text{liver}}) * (\frac{C_{\text{liver}}}{P_{\text{liver}}}) \tag{2.6}$$

where:

M_{ven}	=	total mass of compound in venous blood (μmol);
Q_{t}	=	blood flow from the tissues to venous blood (L/h);
C_{t}	=	concentration of compound in tissue (μmol/L);
P_{t}	=	tissue:blood partitioning coefficient for compound(-);
Q_{gut}	=	blood flow to the gut (L/h);
Q_{liver}	=	blood flow to the liver (L/h);
C_{liver}	=	concentration of the compound in the liver (μmol/L tissue);
P_{liver}	=	liver:blood partitioning coefficient for compound (-).

The concentration in the venous blood can then be calculated by dividing the mass flow of the compound by the total cardiac output (see Equation 2.7). For the venous blood, the same assumption is made as is the case for the arterial blood. Therefore, there is no distinction made between the venous blood leaving the organs and the venous blood entering the heart.

$$C_{\text{ven}} = \frac{M_{\text{ven}}}{Q_{\text{tot}}} \tag{2.7}$$

where:

C_{ven}	=	concentration of compound in venous blood leaving the organs (μmol/L);
M_{ven}	=	total mass of compound in venous blood (μmol);
Q_{tot}	=	cardiac output (L/h).

Gastrointestinal Tract

The gastrointestinal tract is divided into two sub-compartments: the gut lumen and the gut tissue. Each sub-compartment plays a separate role in processing compounds. The gut lumen plays a role in enterohepatic circulation and the metabolism of compounds, while the gut tissue is important for the distribution of compounds from the gut to the liver. Therefore, individual mathematical equations are developed for each of the two sub-compartments.

Gut Lumen

The first sub-compartment of the gastrointestinal tract is the gut lumen. The change in the amount of compound in the gut lumen ($\frac{dM_{\text{lumen}}}{dt}$) is dependent on multiple processes. This is shown in Equation 2.8. The amount of compound entering the gut lumen is determined by the amount of food flowing into the gut lumen from the stomach (Q_{food}) and the concentration of the compound in this food (C_{intake}). The conjugated compound also enters the gut lumen with the bile, of which a fraction can be transformed back into the parent compound for enterohepatic circulation (f_{bact}).

The amount of compound that leaves the gut lumen is a combination of the amount taken up by the gut tissue ($M_{\text{lumen}} * k_{\text{abs}}$) and the amount of compound excreted with the feces ($M_{\text{lumen}} * k_{\text{gastric}}$). In the gut lumen, metabolism is negligible and therefore not taken into account in the current generic PBK model.

$$\begin{aligned}\frac{dM_{\text{lumen}}}{dt} =& Q_{\text{food}} * C_{\text{intake}} + f_{\text{bact}} * f_{\text{bile}} * (Cl_{\text{hepatic}} * C_{\text{liver}}) \\ & - M_{\text{lumen}} * (k_{\text{abs}} + k_{\text{gastric}})\end{aligned} \tag{2.8}$$

where:

$\frac{dM_{\text{lumen}}}{dt}$	=	change in amount of compound in the gut lumen (μmol/h);
Q_{food}	=	food flow from stomach to intestine (L/h);
C_{intake}	=	concentration of compound in food flow (μmol/L);
f_{bact}	=	fraction of conjugate that is transformed back into parent compound in the gut lumen (-);
f_{bile}	=	fraction of conjugate that flows into bile (-);
Cl_{hepatic}	=	hepatic clearance rate (L/h);
C_{liver}	=	concentration of compound in liver (μmol/L);
M_{lumen}	=	amount of compound in the gastrointestinal lumen (μmol);
k_{abs}	=	absorption rate of compound into gut tissue (h^{-1});
k_{gastric}	=	gastric emptying rate (h^{-1}).

Gut Tissue

The second sub-compartment of the gastrointestinal tract is the gut tissue. The change in amount of the compound in the gut tissue ($\frac{dM_{\text{gut}}}{dt}$) is determined by the general equation (Equation 2.2) applied to the gut tissue and the addition of the amount of compound absorbed from the gut lumen ($M_{\text{lumen}} * k_{\text{abs}}$). Equation 2.9 shows this change in compound in the gut tissue.

$$\frac{dM_{\text{gut}}}{dt} = Q_{\text{gut}} * (C_{\text{art}} - \frac{C_{\text{gut}}}{P_{\text{gut}}}) + M_{\text{lumen}} * k_{\text{abs}} \tag{2.9}$$

where:

$\frac{dM_{\text{gut}}}{dt}$	=	change in amount of compound in the gut tissue (μmol/h);
Q_{gut}	=	blood flow to the gut (L/h);
C_{art}	=	concentration of compound in arterial blood flowing to the gut (μmol/L);
C_{gut}	=	concentration of compound in gut (μmol/L);
P_{gut}	=	gut:blood partitioning coefficient for compound (-);
M_{lumen}	=	amount of compound in the gastrointestinal lumen (μmol);
k_{abs}	=	absorption rate of compound into gut tissue (h^{-1}).

Liver

The next compartment in the current PBK model is the liver. The liver is considered the most important metabolizing organ. The blood flow around the liver consists of the portal vein (Q_{gut}), flowing from the gut to the liver, and the hepatic artery (Q_{liver}). The compound often gets excreted out of the liver in the form of conjugates, via the bile into the gut lumen (f_{bile} in Equation 2.9). The change in the amount of compound in the liver over time ($\frac{dM_{\text{liver}}}{dt}$) is shown in Equation 2.10.

Part of the conjugates that are excreted out of the liver with the bile, may be subject to enterohepatic circulation. The process of enterohepatic circulation is described in Section 2.2. The conjugates are metabolized back into the original parent compound and are recycled back to the liver through the portal vein. This is shown as f_{bact} in Equation 2.8.

$$\begin{aligned}\frac{dM_{\text{liver}}}{dt} =& Q_{\text{liver}} * (C_{\text{art}} - \frac{C_{\text{liver}}}{P_{\text{liver}}}) \\ & - Cl_{\text{hepatic}} * C_{\text{liver}} \\ & + Q_{\text{gut}} * (\frac{C_{\text{gut}}}{P_{\text{gut}}}) - Q_{\text{gut}} * (\frac{C_{\text{liver}}}{P_{\text{liver}}})\end{aligned} \tag{2.10}$$

where:

$\frac{dM_{\text{liver}}}{dt}$	=	change in the amount of compound in the liver (μmol/h);
Q_{liver}	=	blood flow to the liver (L/h);
C_{art}	=	concentration of the compound in the arterial blood flowing to the liver (μmol/L);
C_{liver}	=	concentration of the compound in the liver (μmol/L);
P_{liver}	=	liver:blood partitioning coefficient for compound (-);
Cl_{hepatic}	=	hepatic clearance rate (L/h);
Q_{gut}	=	blood flow from the gut tissue (L/h);
C_{gut}	=	concentration of the compound in the gut tissue (μmol/L);
P_{gut}	=	gut tissue:blood partitioning coefficient for the compound (-).

Kidney

The kidney excretes compound from the body. The change in the amount of compound in the kidney ($\frac{dM_{\text{kidney}}}{dt}$) is therefore shown as the general mass balance, combined with a term for excretion ($C_{\text{kidney}} * Cl_{\text{renal}}$). This leads to Equation 2.11.

$$\frac{dM_{\text{kidney}}}{dt} = Q_{\text{kidney}} * (C_{\text{art}} - \frac{C_{\text{kidney}}}{P_{\text{kidney}}}) - (C_{\text{kidney}} * Cl_{\text{renal}}) \tag{2.11}$$

where:

$\frac{dM_{\text{kidney}}}{dt}$	=	change in amount of compound in the kidney (μmol/h);
Q_{kidney}	=	blood flow to the kidney (L/h);
C_{art}	=	concentration of the compound in the arterial blood to the kidney (μmol/L);
C_{kidney}	=	concentration of the compound in the kidney (μmol/L);
P_{kidney}	=	kidney:blood partitioning coefficient of the compound (-);
Cl_{renal}	=	renal clearance rate (L/h).

Lungs

In the current generic PBK model, the lungs are sources of metabolism and excretion of compounds. Exposure through inhalation is not taken into account in the model. In Equation 2.12, the pulmonary blood flow is represented. This is in contrast to the bronchial blood flow, that is part of the remainder of the body and can be determined with Equation 2.1. The pulmonary blood flow consists of the pulmonary artery, that flows from the heart to the lungs and is low in oxygen, and the pulmonary vein, that flows from the lungs to the heart and is rich in oxygen. From the heart the oxygen-rich blood is then distributed to the remainder of the body.

$$\begin{aligned}\frac{dM_{\text{lung}}}{dt} =& Q_{\text{tot}} * (C_{\text{lven}} - C_{\text{lart}}) \\ & - \frac{Q_{\text{exhale}} * P_{\text{air}}}{Q_{\text{tot}} + Q_{\text{exhale}} * P_{\text{air}}}\end{aligned} \tag{2.12}$$

where:

$\frac{dM_{\text{lung}}}{dt}$	=	change in amount of compound in the lung (μmol/h);
Q_{tot}	=	cardiac output (L/h);
C_{lven}	=	concentration of compound in venous blood entering lungs (μmol/L);
C_{lart}	=	concentration of compound in arterial blood leaving lungs (μmol/L);
Q_{exhale}	=	mammalian ventilation rate (L/h);
P_{air}	=	lung:blood partitioning coefficient of the compound (-);

Mammary Gland and Lumped Reproductive Organs

Another route of excretion is through the mammary gland and lumped reproductive organs. In the current model, the mammary gland (and milk production) are taken into consideration for cattle and sheep. For chicken, excretion through the production of eggs was included in the model.

Mammary Gland

Mammals produce milk, which can be a route of excretion for compounds. As this milk is used in many (consumer) products, it is important for food safety to have knowledge on this route of exposure. Equation 2.13 shows that the change in the amount of compound in the mammary gland ($\frac{dM_{\text{mgland}}}{dt}$) can be described by the general mass balance, in addition to a factor describing the excretion ($Q_{\text{milk}} * C_{\text{mgland}}$).

$$\frac{dM_{\text{mgland}}}{dt} = Q_{\text{mgland}} * (C_{\text{art}} - \frac{C_{\text{mgland}}}{P_{\text{mgland}}}) - (Q_{\text{milk}} * C_{\text{mgland}}) \tag{2.13}$$

where:

$\frac{dM_{\text{mgland}}}{dt}$	=	change in amount of compound in the mammary gland (μmol/h);
Q_{mgland}	=	blood flow rate to mammary gland (L/h);
C_{art}	=	concentration of compound in arterial blood to mammary gland (μmol/L);
C_{mgland}	=	concentration of compound in mammary gland (μmol/L);
P_{mgland}	=	mammary gland:blood partitioning coefficient for compound (-);
Q_{milk}	=	flow rate of milk (L/h).

Eggs

Chickens do not produce milk, but they do produce eggs. These eggs are also used for consumption and therefore are also important to be taken into consideration for food safety. The mass balance for the production of eggs is similar to the mass balance for milk production. Equation 2.14 shows that to determine the change in the amount of compound in the reproductive system ($\frac{dM_{\text{rep}}}{dt}$) the general mass balance is needed, in addition to a term for the excretion of the compound through eggs ($Q_{\text{egg}} * C_{\text{rep}}$).

$$\frac{dM_{\text{rep}}}{dt} = Q_{\text{rep}} * (C_{\text{art}} - \frac{C_{\text{rep}}}{P_{\text{egg}}}) - (Q_{\text{egg}} * C_{\text{rep}}) \tag{2.14}$$

where:

$\frac{dM_{\text{rep}}}{dt}$	=	change in the amount of compound in the reproductive system (μmol/h);
Q_{rep}	=	blood flow rate to the reproductive system (L/h);
C_{art}	=	concentration of the compound in the arterial blood flow to reproductive system (μmol/L);
C_{rep}	=	concentration of the compound in the reproductive system (μmol/L);
P_{egg}	=	egg:blood partitioning coefficient for the compound (-);
Q_{egg}	=	egg production rate (L/h).

Chapter 3

Goat-specific Adaptation of Current PBK Model

The current PBK model, as developed by Lautz et al. (2017), can be used for cattle, sheep, swine and chicken. However, the goal of this thesis is to adjust and parameterize this model, in order for it to accurately describe the internal dose of different compounds in goats. In this chapter, the goat-specific physiological parameters and values will be elaborated on and implemented into the model. Necessary assumptions are also explained in this chapter.

3.1 Goat-Adjusted Model Compartments

In order to adjust the current generic PBK model to fit the goat, there are specific physiological parameters which must be implemented or excluded from the current model. Literature studies have shown which compartments, and corresponding physiological parameters, are of importance for the goat. Like sheep and cattle, goats are a ruminant species, meaning their stomach consists of four compartments. These four compartments replace the 'stomach' compartment of the generic model (Section 2.1).

The gizzard and crop were also removed for the goat-adjusted PBK model, as goats do not have these organs. In the generic model by Lautz et al. (2017), the lumped reproduction organs are only applicable to chickens. Therefore, the assumption is made that this compartment is not applicable to goats. For the goat-adjusted PBK model, the following selection of compartments from the current model (see Section 2.1) is needed:

- ruminant stomach, consisting of:
  - rumen;
  - reticulum;
  - omasum;
  - abomasum;
- intestine;
- liver;
- kidney;
- heart;
- brain;
- lung;
- blood;
- mammary gland;
- fat; and
- muscle.

For each of the compartments, multiple physiological parameters must be included in the model. This can be verified by the previously mentioned equations (see Section 2.2.2). These parameters include the weight and blood flow fractions of target organs. The values that are implemented in the goat-specific model, are detailed in Section 3.2.

3.2 Model Values for Implementation

In this section, the values of the physiological parameters, as implemented into the goat-specific PBK model, are given. These values were derived from multiple literature studies. For several compartments,

only one value was found. However, for other parameters, multiple studies were available. To establish the input distribution, the found data had to be combined. Equation 3.1 shows how data were combined, using the method developed by Ragas and Huijbregts (1998). In this method, the arithmetic means and standard deviations are combined, based on the sample size of the respective studies (Lautz et al., 2017; Ragas & Huijbregts, 1998). The squared standard deviation (SD^2) of the combined studies, is calculated using Equation 3.2.

$$G_{\text{combined}} = \frac{\sum_{x=1}^{x=n} N_{\text{x}} * G_{\text{x}}}{\sum_{x=1}^{x=n} N_{\text{x}}} \tag{3.1}$$

where:

G_{combined}	=	combined mean of two or more studies x;
N_{x}	=	sample size of study x;
G_{x}	=	mean of the individual study x;
n	=	number of studies to be combined.

$$\begin{aligned} SD^2_{combined} = & \frac{1}{(\sum_{x=1}^{x=n} N_{\text{x}}) - 1} * \\ & (\sum_{x=1}^{x=n} [(N_{\text{x}} - 1) * SD_x^2 + N_{\text{x}} * G_x^2 \\ & - 2 * N_{\text{x}} * G_{\text{x}} * G_{\text{combined}} + N_{\text{x}} * G^2_{combined}]) \end{aligned} \tag{3.2}$$

where:

$SD^2_{combined}$	=	combined squared standard deviation of studies x;
SD_x^2	=	squared standard deviation of study x.

3.2.1 Assumptions

Several assumptions were made for the goat-adjusted PBK model. These assumptions are necessary to have a working model. This section elaborates which assumptions were made and why these specific choices were made. For the following topics, assumptions were made for the goat-adjusted model:

1. allometric scaling;
2. tissue composition parameters for mammals; and
3. the use of sheep data.

Allometric Scaling

The first subject is the use of allometric scaling in the goat-adjusted PBK model. There are two equations that describe the allometric relationships. The first being an exponential equation (Equation 3.3). One can also make a linear equation out of this, after a logarithmic transformation, leading to Equation 3.4 (Lautz et al., 2017).

$$Y = a * W^b \tag{3.3}$$

$$\log Y = \log a + b * \log W \tag{3.4}$$

where:

Y	=	parameter under study;
a	=	allometric coefficient (intercept of the linear equation);
W	=	body weight of the species (kg);
b	=	allometric exponent (slope of the linear equation).

In the specific case where the values for Y_s and W_s are known for one species, and the weight (W_n) of the species of interest is known, one can rewrite Equation 3.3 into Equation 3.5:

$$Y_n = (\frac{W_s}{W_n})^{1-b} * Y_s \tag{3.5}$$

where:

Y_n	=	parameter under study of the species of interest;
W_n	=	body weight of the species of interest (kg);
Y_s	=	experimental value of the parameter under study for another species that is used as a basis for extrapolation;
W_s	=	body weight of the other species that is used for extrapolation (kg).

Not all compounds qualify for allometric scaling. Lautz et al. (2017) argue that compounds that are mainly excreted through renal clearance, do qualify for allometric scaling. This is due to the well documented knowledge on renal physiology for many mammals. However, compounds that are excreted through hepatic clearance should not be used in allometric scaling, as the hepatic metabolism differs significantly between species (Lautz et al., 2017). This limits the amount of compounds that can be used for the validation of the goat-adjusted PBK model. An exception to this, is when it is ensured that at least 80% of the compound is excreted through renal clearance.

The availability of compounds that were tested on multiple tissues of goats is limited. Therefore, some toxicokinetic data (available in Table 4.2) was extrapolated from available data of other species using allometric scaling. For two out of three of the chosen validation studies, the absorption coefficient (k_{abs}), renal and hepatic clearance rates were extrapolated from data of sheep and cattle. Section 4.1 specifically shows which parameters were scaled from other species.

Tissue Composition Parameters for Mammals

The model uses tissue composition parameter values for its calculations. It is assumed that these values are the same for all mammals. This is due to a lack of data showing otherwise. In the goat-adjusted PBK model, the parameter values are therefore kept the same as in the original PBK model. These values are given in Table 3.1.

Use of Sheep Data

Besides toxicokinetic data, physiological data of the sheep is also used in the goat-adjusted PBK model. This model assumes that the physiology of goat and sheep are sufficiently similar and physiological data of the sheep can therefore be used in the goat-adjusted model when necessary. This is the case for compartments whose weight is described as a fraction of the body weight, or blood flow which is described as a fraction of the cardiac output and/or weight of the relevant organ (Table 3.2).

These are the most important assumptions made for this goat-adjusted PBK model. The combination of these assumptions leads to the model, which will be tested and validated in Chapter 4.

3.2.2 Physiological Parameters

Table 3.1 shows the different tissue composition parameters for the goat. There are four values taken into consideration, namely the fractions of neutral lipids, polar lipids, proteins and water. As described in 3.2.1, it is assumed that these values are the same for all mammals. Another parameter is the food intake rate. For the goat (all sexes) it was assumed the same as for sheep, namely 4.77 kg/day (Lautz et al., 2017).

Also important is the gastric emptying rate ($k_{gastric}$), which is set, for all sexes, at $2.083*10^{-3}$ min^{-1}. This value is based on personal communication with Ad Ragas. It is assumed that the average time a compound stays in the gastrointestinal tract is 8 hours. This leads to a removal of 300% per day, meaning $k_{gastric}$ is 3 per day and therefore $2.083*10^{-3}$ per minute.

Using Equations 3.1 and 3.2, the physiological parameter values for the goat-specific PBK model were calculated. These values are shown in Table 3.2. They are based on literature studies. Several of the values in Table 3.2 are based on values found for sheep, as explained in Section 3.2.1.

Table 3.2 shows three values per parameter, one for each sex and a combined (mixed) value. This distinction was made so users of the model can decide which values best fit their goal. In a test using both sexes, the combined value can be used, while one can also view the effects of compounds on a specific sex. The latter can be useful, for example, when determining the effects of a compound on the milk produced by the female goat.

Three comments about the values in Table 3.2 must be made, namely:

1. the fractions do not add up to 1.00. However, the model normalizes the values of the fractions to add up to 1.00;
2. the fraction of body weight for the carcass weight was reduced from 0.51, 0.48 and 0.51 for the male, female and mixed goats respectively, to 0.31 to avoid double calculations of part of the muscle and fat weight;
3. when data was not available in scientific literature, the assumption was made that the values for the compartments between sexes are proportional. Meaning the ratio between male and female for one compartment, is similar to the ratio between male and female for another compartment. This assumption was used to calculate the missing values (which therefore do not have a reference).

The second point needs more elaboration. In literature found, the carcass weight consists of muscle, bone and adipose tissue. Muscle and fat are considered separate compartments in the PBK model. Therefore, the fraction of body weight for the carcass weight needs to be adjusted so muscle and fat are not counted double in the total body weight. The values were reduced from a fraction of 0.51, 0.48 and 0.51 for male goats, female goats and mixed goats respectively, to a body weight fraction of 0.31 for the carcass. Before the reduction, the total of all body weight fractions, was around 1.20. The assumption was made that the value above 1.00 was for a large part caused by the muscle and adipose tissue being counted double. Therefore, the adjustment was made, leading to the carcass weight fraction being 0.31.

Table 3.1: Tissue Composition Parameters for Goat (Lautz et al., 2017).

Compartment	**Fraction of Neutral Lipids**	**Fraction of Polar Lipids**	**Fraction of Proteins**	**Fraction of Water**
Fat	0.794	0.000	0.057	0.157
Brain	0.043	0.067	0.080	0.790
Carcass	0.017	0.003	0.193	0.328
Heart	0.047	0.051	0.169	0.734
Intestine	0.045	0.020	0.139	0.792
Kidney	0.013	0.038	0.173	0.776
Liver	0.020	0.049	0.179	0.727
Lung	0.015	0.036	0.125	0.84
Muscle	0.005	0.006	0.172	0.782
Mammary gland	0.042	0.0004	0.035	0.872
Blood	0.005	0.011	0.168	0.804

Table 3.2: Physiological parameter values ± SD and units for goat-adjusted PBK model. Values for male, female and mixed options.

Parameter	**Male**	**Female**	**Mixed**	**Unit**
Body weight	19.20 ± 4.710[1,2,3,5]	16.80 ± 4.750[2,3,5]	17.80 ± 4.760[1,2,3,4,5]	kg
Cardiac output	4.500[a,15]	4.970 ± 1.200[a,7,8,11,12]	4.890 ± 1.090[a,6,13]	L/min
Heart rate	96.38 ± 10.77[a,15]	77.05 ± 14.16[a,7,11]	80.08 ± 16.56[a,13]	beats/min
Respiratory frequency	19.69 ± 3.200[a,15]	122.6 ± 12.56[a,7]	74.82 ± 53.08[a]	breaths/min
Carcass weight	0.3100 ± 0.1520[1,2,3,5,17]	0.3100 ± 0.1630[2,3,5]	0.3100 ± 0.1580[1,2,3,4,5,6]	fraction BW
Blood weight	0.1520[1]	0.1520 ± 0.0180[12,19]	0.1520[1]	fraction BW
Heart weight	0.0050 ± 0.0005[1,2,3,5]	0.0030 ± 0.0003[2,3,5,7]	0.0030 ± 0.0003[1,2,3,4,5,16]	fraction BW
Lung + Trachea weight	0.0100 ± 0.0014[1,2,3,5]	0.0100 ± 0.0011[2,3,5]	0.0100 ± 0.0009[1,2,3,4,5]	fraction BW
Brain weight	0.0030[a,21]	0.0030[a,21]	0.0030 ±[a,21]	fraction BW
Muscle weight	0.3500 ± 0.0140[2,3,5]	0.3200 ± 0.0050[2,3,5]	0.3400 ± 0.0140[2,3,4,5]	fraction BW
Fat weight	0.0700 ± 0.0140[1,2,3,5]	0.0700 ± 0.0040[2,3,5]	0.0700 ± 0.0130[1,2,3,4,5,6]	fraction BW
Abomasal weight	0.0050 ± 0.0020[a,21]	0.0050 ± 0.0020[a,21]	0.0050 ± 0.0020[a,21]	fraction BW
Omasal weight	0.0020 ± 0.0010[a,21]	0.0020 ± 0.0010[a,21]	0.0020 ± 0.0010[a,21]	fraction BW
Rumenal weight	0.0110 ± 0.0020[a,21]	0.0110 ± 0.0020[a,21]	0.0110 ± 0.0020[a,21]	fraction BW
Reticular weight	0.0020 ± 0.0004[a,21]	0.0020 ± 0.0004[a,21]	0.0020 ± 0.0004[a,21]	fraction BW
Intestinal weight	0.0700 ± 0.0110[1,2,3,5,17]	0.0400 ± 0.0060[2,3,5]	0.0400 ± 0.0060[1,2,3,4,5]	fraction BW
Liver weight	0.0200 ± 0.0025[1,2,3,5,17]	0.0100 ± 0.0008[2,3,5,7]	0.0100 ± 0.0016[1,2,3,4,5]	fraction BW
Kidney weight	0.0030 ± 0.0002[a,1,17]	0.0030[a,7]	0.0030[a,1,16]	fraction BW
Mammary gland weight	-	0.0460 ± 0.0130[18]	-	fraction BW
Carcass blood flow	0.1210 ± 0.0510[21]	0.1210 ± 0.0510[21]	0.1210 ± 0.0510[21]	fraction CO
Cardiac blood flow	0.0284 ± 0.0064[a,15]	0.0102 ± 0.0020[a,7]	0.0117 ± 0.0047[a,16]	fraction CO
Pulmonary blood flow	0.0002[10]	0.0002[10]	0.0002[10]	fraction CO
Cerebral blood flow	0.0074 ± 0.0008[15]	0.0056 ± 0.0007[7,8,9]	0.0064 ± 0.0008	fraction CO
Muscular blood flow	0.3571 ± 0.0782[a]	0.3006 ± 0.1610[a,8]	0.3313 ± 0.1276[a]	fraction CO
Fat blood flow	0.0220 ± 0.0060[a,21]	0.0220 ± 0.0060[a,21]	0.0220 ± 0.0060[a,21]	fraction CO
Abomasal blood flow	0.0370 ± 0.0200[a,21]	0.0370 ± 0.0200[a,21]	0.0370 ± 0.0200[a,21]	fraction CO
Omasal blood flow	0.0090 ± 0.0040[a,21]	0.0090 ± 0.0040[a,21]	0.0090 ± 0.0040[a,21]	fraction CO
Rumenal blood flow	0.0650 ± 0.0420[a,21]	0.0650 ± 0.0420[a,21]	0.0650 ± 0.0420[a,21]	fraction CO
Reticular blood flow	0.0080 ± 0.0060[a,21]	0.0080 ± 0.0060[a,21]	0.0080 ± 0.0060[a,21]	fraction CO
Intestinal blood flow	0.1448[a,15]	0.0836 ± 0.0194[a,7,8]	0.0848[a]	fraction CO
Hepatic blood flow	0.0032 ± 0.0006	0.0015 ± 0.0007[7,8]	0.0018 ± 0.0006[14]	fraction CO
Renal blood flow	0.0690 ± 0.0114[15]	0.0679 ± 0.0275[7,8,11]	0.0690 ± 0.0194[16]	fraction CO
Mammary gland blood flow	-	0.0637 ± 0.0146[18]	-	fraction CO
Milk production	-	$1.107*10^{-3}$ ± $5.42*10^{-5}$ [20]	-	L/min

[a] Retrieved from sheep data.
[1] Ngwa et al. (2009)
[2] Mahgoub (1997)
[3] Mahgoub & Lodge (1996)
[4] Mahgoub & Lodge (1998)
[5] Mahgoub & Lu (1998)
[6] Gregory et al. (1986)
[7] Hales & Fawcett (1993)
[8] Talke et al. (2000)
[9] Pelligrino et al. (1984)
[10] Melsom et al. (1995)
[11] Ullman et al. (2001)
[12] Norberg et al. (2005)
[13] Di Giantomasso et al. (2004)
[14] Kisauzi & Leek (1991)
[15] Hales (1973)
[16] Barnes et al. (1983)
[17] Burrin et al. (1990)
[18] Linzell (1960)
[19] Grimes et al. (1987)
[20] Peris et al. (1999)
[21] Lautz et al. (2017)

Chapter 4

Model Validation

In this chapter the goat-adjusted PBK model will be validated. First, a selection is made of model validation sets, after which the model will be run. In Sections 4.2 - 4.4, the results of the model will then be compared to the experimental data of the validation sets. The used model code is available in Appendix A and the raw results are available in Appendix B.

4.1 Definition and Selection of Model Validation Sets

The first step in the validation of the goat-adjusted PBK model, is finding literature studies that can be used for this purpose. An extensive literature search, using Google Scholar, was done in order to identify suitable case studies. An important criterion for a study to be usable, is that it describes the tissue distribution of the chemical in the goat, preferably in multiple tissues such as blood, urine, liver, etc. Only a few studies were available that meet this criterion.

More specifically, only two valid studies were found that describe the tissue distribution of chemicals within the goat. The first study is about the anti-parasitic medication ivermectin. In this study, a dosage of 0.2 mg ivermectin per kilogram body weight was given to 9 male goats orally (Lespine et al., 2005). Ivermectin concentrations were measured in plasma, hair, fat, skin, lung, liver, intestinal mucosa and abomasal mucosa at 2, 7 and 17 days after exposure.

The second case study is about another antibiotic, namely chloramphenicol. In this study, a gender-mixed group of 24 goats was intravenously dosed with 25 mg chloramphenicol per kilogram of bodyweight (Etuk & Onyeyili, 2005b). Chloramphenicol concentrations were measured in liver, skeletal muscle, brain, lungs, kidney, spleen and bone marrow at 11 points in time starting at 0.08 hours until 240 hours after exposure. More extensive information on the studies, is given in Sections 4.2 and 4.3.

Neither of the above-mentioned studies gave results on the distribution of the chemical in the milk of the goat. No case study was found that described both the distribution of the compound in tissues as well as in milk. As the production of goat milk is also important, the decision was made to add a third case study, which focuses specifically on the distribution of the compound in the milk. For this, a study using the antibiotic moxifloxacin was used. In this study, a dosage of 5 mg of moxifloxacin per kilogram of body weight was given to 6 female goats (Fernandez-Varon et al., 2006). More thorough information on this study is given in Section 4.4.

The combination of these three case studies, covers the distribution in as many tissues as possible. The choices also reflect the three possibilities for inclusion of gender in the model, namely male, female and mixed, as is described in Section 3.2.2. Therefore, these studies include as many different validation factors as possible, making them a good set to validate the goat-adjust PBK model.

After these case studies were selected, a literature search was performed to find the chemical specific properties and toxicokinetic parameters of the three compounds. This data is given in Tables 4.1 and 4.2. Table 4.1 shows the chemical specific properties for the three compounds used for the validation of the goat-adjusted PBK model. Table 4.2 shows the toxicokinetic parameters and rates of these compounds. These include the absorption rate into the gut tissue (k_{abs}), the renal and hepatic clearance rates (Cl_{renal} and $Cl_{hepatic}$ respectively).

Several of the values in 4.2 were calculated based on allometric scaling, as is described in Section 3.2.1.

For ivermectin, k_{abs} was extrapolated from sheep data, using the study by Mestorino et al. (2003). A body weight for the sheep (W_s in Equation 3.5) of 60 kg was used for the allometric scaling here. Both the renal and hepatic clearance are based on cattle data from the study by Lanusse et al. (1997). Here a body weight for the cattle of 210 kg was used. The allometric exponent (b in Equation 3.5) was set at 0.75, based on the study by Duthaler et al. (2020).

For moxifloxacin, k_{abs} and both clearance rates were extrapolated from data of the sheep, using the study by Goudah (2008). A body weight of 45 kg was used for the sheep. The allometric exponent was set at 0.8805 based on a study by Huang et al. (2015).

Table 4.1: Chemical specific properties.

Chemical	**Molecular Weight (g/mole)**	**Solubility (mg/L at 25°C)**	**Vapor Pressure (Pa)**	**K_{ow} (-)**	**Reference**
Ivermectin	874.7	4	$1.50*10^{-9}$	1584.89	Liebig et al. (2010)
Chloramphenicol	323.13	2500	$2.27*10^{-10}$	13.8	EFSA (2014)
Moxifloxacin	401.4	1146	$9.68*10^{-13}$	8.91	NCBI, n.d.

Table 4.2: Toxicokinetic parameters and rates.

Chemical	Sex	**k_{abs} (min^{-1})**	**Cl_{renal} (L/min)**	**$Cl_{hepatic}$ (L/min)**	**References**
Ivermectin	Male	0.002 [a]	$1.15*10^{-5}$ [b]	$5.66*10^{-4}$ [b]	Duthaler et al. (2020), Lanusse et al. (1997), Mestorino et al. (2003)
Ivermectin	Female	0.0032 [c]	$1.19*10^{-5}$ [d]	$5.85*10^{-4}$ [d]	Duthaler et al. (2020), Lanusse et al. (1997), Mestorino et al. (2003)
Ivermectin	Mixed	0.0029 [e]	$1.18*10^{-5}$ [f]	$5.76*10^{-4}$ [f]	Duthaler et al. (2020), Lanusse et al. (1997), Mestorino et al. (2003)
Chloramphenicol	Male	0.0889	0.0133	0.00	Etuk & Onyeyili (2005a)
Chloramphenicol	Female	0.0889	0.0133	0.00	Etuk & Onyeyili (2005a)
Chloramphenicol	Mixed	0.0889	0.0133	0.00	Etuk & Onyeyili (2005a)
Moxifloxacin	Male	0.128 [g]	0.001 [g]	0.005 [g]	Goudah (2008), Huang et al. (2015)
Moxifloxacin	Female	0.140 [h]	0.001 [h]	0.005 [h]	Goudah (2008), Huang et al. (2015)
Moxifloxacin	Mixed	0.132 [i]	0.001 [i]	0.005 [i]	Goudah (2008), Huang et al. (2015)

[a] Extrapolated from sheep using an extrapolation factor of 0.75 and a body weight of 60 kg for sheep and of 19.2 kg for goat.
[b] Extrapolated from cattle using an extrapolation factor of 0.75 and a body weight of 210 kg for cattle and of 19.2 kg for goat.
[c] Extrapolated from sheep using an extrapolation factor of 0.75 and a body weight of 60 kg for sheep and of 16.8 kg for goat.
[d] Extrapolated from cattle using an extrapolation factor of 0.75 and a body weight of 210 kg for cattle and of 16.8 kg for goat.
[e] Extrapolated from sheep using an extrapolation factor of 0.75 and a body weight of 60 kg for sheep and of 17.8 kg for goat.
[f] Extrapolated from cattle using an extrapolation factor of 0.75 and a body weight of 210 kg for cattle and of 17.8 kg for goat.
[g] Extrapolated from sheep using an extrapolation factor of 0.8805 and a body weight of 45 kg for sheep and of 19.2 kg for goat.
[h] Extrapolated from sheep using an extrapolation factor of 0.8805 and a body weight of 45 kg for sheep and of 16.8 kg for goat.
[i] Extrapolated from sheep using an extrapolation factor of 0.8805 and a body weight of 45 kg for sheep and of 17.8 kg for goat.

4.2 Case Study Ivermectin

4.2.1 Description of Compound

Ivermectin is part of the avermectins, which are macrocyclic lactones. Avermectins are broadly used, as they are effective against a large number of nematodes, mites and insects. Figure 4.1 shows the chemical structure of ivermectin. Ivermectin is an anthelmintic, which is commonly used in livestock, such as goats, sheep and cattle, pets and humans, but also in agriculture to protect fruits and vegetables (Lespine et al., 2005 & Liebig et al., 2010). It can be given orally or subcutaneously, the latter is the more efficient route (Campbell, 1985 & Lespine et al., 2005).

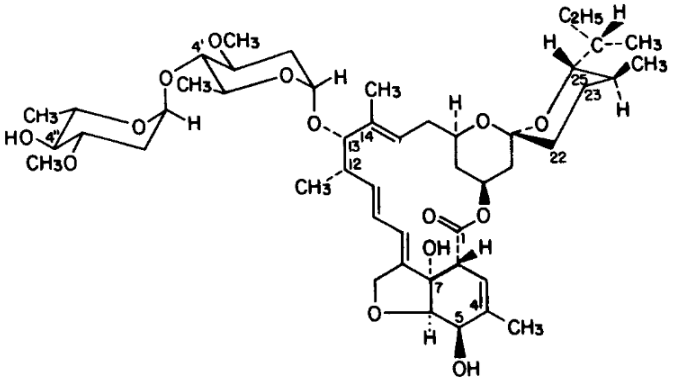

Figure 4.1: Chemical structure of ivermectin (Campbell, 1985).

The hydrophobic pharmaceutical compound binds to lipoproteins in the blood This is how ivermectin distributes itself through the body (Lespine et al., 2005). It is mostly stored in adipose tissue. The amount of ivermectin that is metabolized by the liver, is very low (Lespine et al, 2005). The compound is excreted in the same form as it is applied. The main route of excretion of ivermectin is through the feces, with less than 2% being excreted through the urine (Campbell, 1985; Liebig et al., 2010).

4.2.2 Description of Validation Study

A study performed by Lespine et al. (2005) was used for validation. The goal of this study was to compare the efficiency of ivermectin in goats, after oral and subcutaneous administration, in the same supplied dosage. For the validation of the goat-adjusted PBK model, only the data of the orally exposed goats were used. A total of 24 male French Alpine goats, weighing between 16 and 23 kilograms, were used for this study. Nine of these goats were given an oral dosage of 0.2 mg ivermectin per kilogram body weight. Three of the goats were sacrificed at 2, 7 and 17 days, after which blood and tissue sampling took place. The ivermectin concentration was then measured in the plasma and different tissue samples. Tissue samples include: hair, fat, skin, lung, liver, intestine and abomasum.

4.2.3 Results of Model Run

The model simulation of ivermectin was done using the data (as described in Chapter 3) for a male goat, with a 'standardized' body weight of 19.2 kg. Multiple compartments were modeled: blood, fat, lung, liver, intestine and abomasum. Hair and skin were are not included in the model and therefore could not be simulated.

The study by Lespine et al. (2005) shows measured concentrations at 2 days (48 hours), 7 days (168 hours) and 17 days (408 hours) after exposure to ivermectin. The model gave predicted results at 24, 48, 120, 168, 240, 336 and 408 hours after exposure (1, 2, 5, 7, 10, 14 and 17 days). The decision to simulate internal concentrations for the extra time points was made in order to have a better representation of the results. The raw results are shown in Table B.1 in Appendix B.

Figures 4.2 through 4.7 show a comparison of measured and predicted results for the modeled compartments. All compartments, except fat show a similar trend. The predicted and measured concentrations are very similar to each other 48 hours after exposure. At 168 hours after exposure, the difference increases to the measured concentrations being 300 - 1200 times higher than the concentrations the model predicts. For these 5 compartments, concentrations were 'non-detected' at 408 hours after exposure. For the graphs,

the assumption was made that this is a concentration of 0.00 μg/mL.

For fat, the difference between the measured and predicted concentrations is higher than for the other compartments. The measured concentration is 14 times higher than the predicted concentrations at 48 hours after exposure. The difference increases to 6000 times at 168 hours and $1.13*10^{10}$ times at 408 hours after exposure. Fat was the only compartment with a detectable amount of ivermectin at the last measurement.

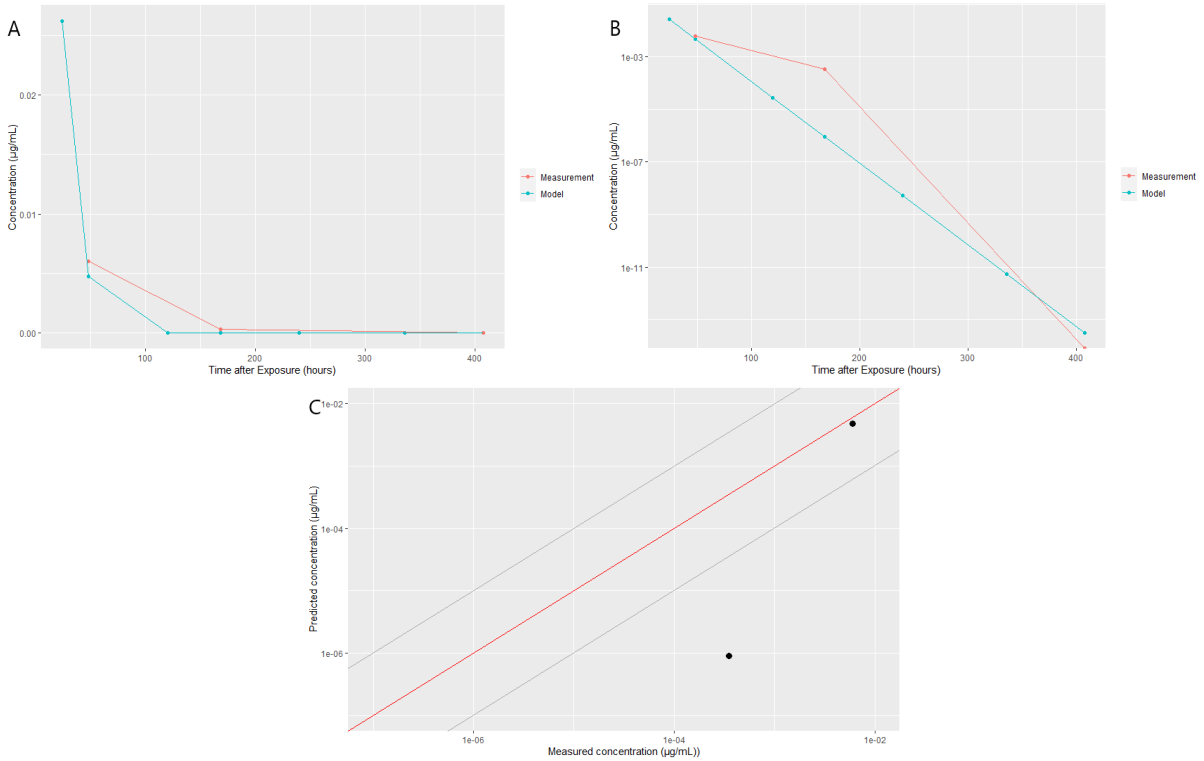

Figure 4.2: Ivermectin concentration in the plasma. (A) Ivermectin concentration over time. (B) Ivermectin concentration over time in a semi-logarithmic plot. (C) Predicted concentrations versus measured concentrations for ivermectin in the plasma. Both axes are on log-scale. The red line shows the 1:1 line when predicted and measured concentrations match perfectly. The gray lines above and below represent a deviation of factor 10 of the 1:1 line.

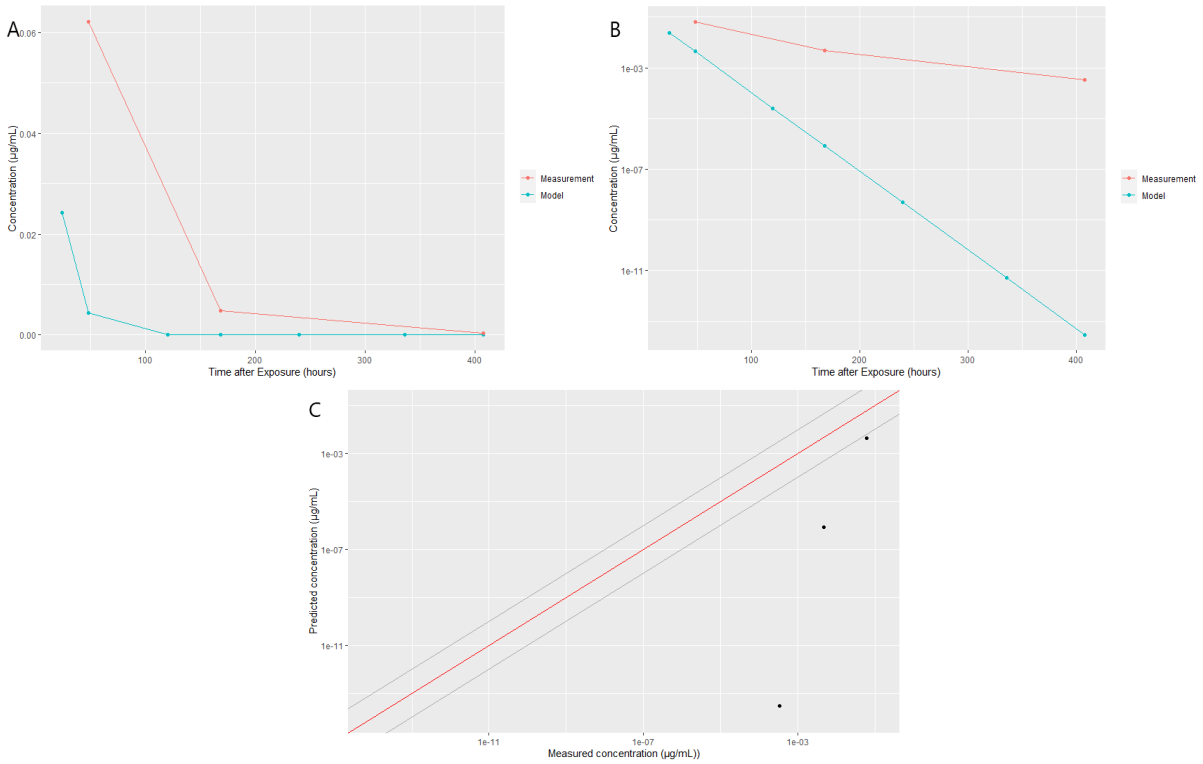

Figure 4.3: Ivermectin in the adipose tissue. (A) Ivermectin concentration over time. (B) Ivermectin concentration over time in a semi-logarithmic plot. (C) Predicted concentrations versus measured concentrations for ivermectin in the adipose tissue. Both axes are on log-scale. The red line shows the 1:1 line when predicted and measured concentrations match perfectly. The gray lines above and below represent a deviation of factor 10 of the 1:1 line.

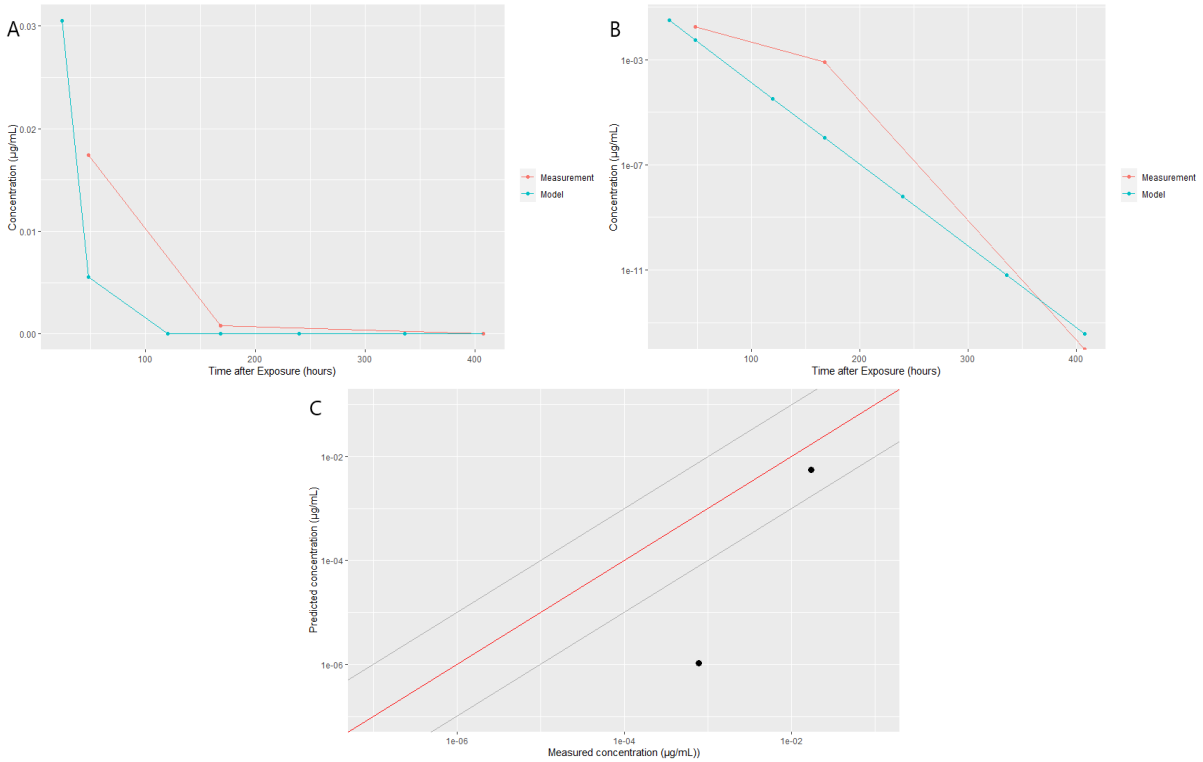

Figure 4.4: Ivermectin in the abomasal mucosa. (A) Ivermectin concentration over time. (B) Ivermectin concentration over time in a semi-logarithmic plot. (C) Predicted concentrations versus measured concentrations for ivermectin in the abomasal mucosa. Both axes are on log-scale. The red line shows the 1:1 line when predicted and measured concentrations match perfectly. The gray lines above and below represent a deviation of factor 10 of the 1:1 line.

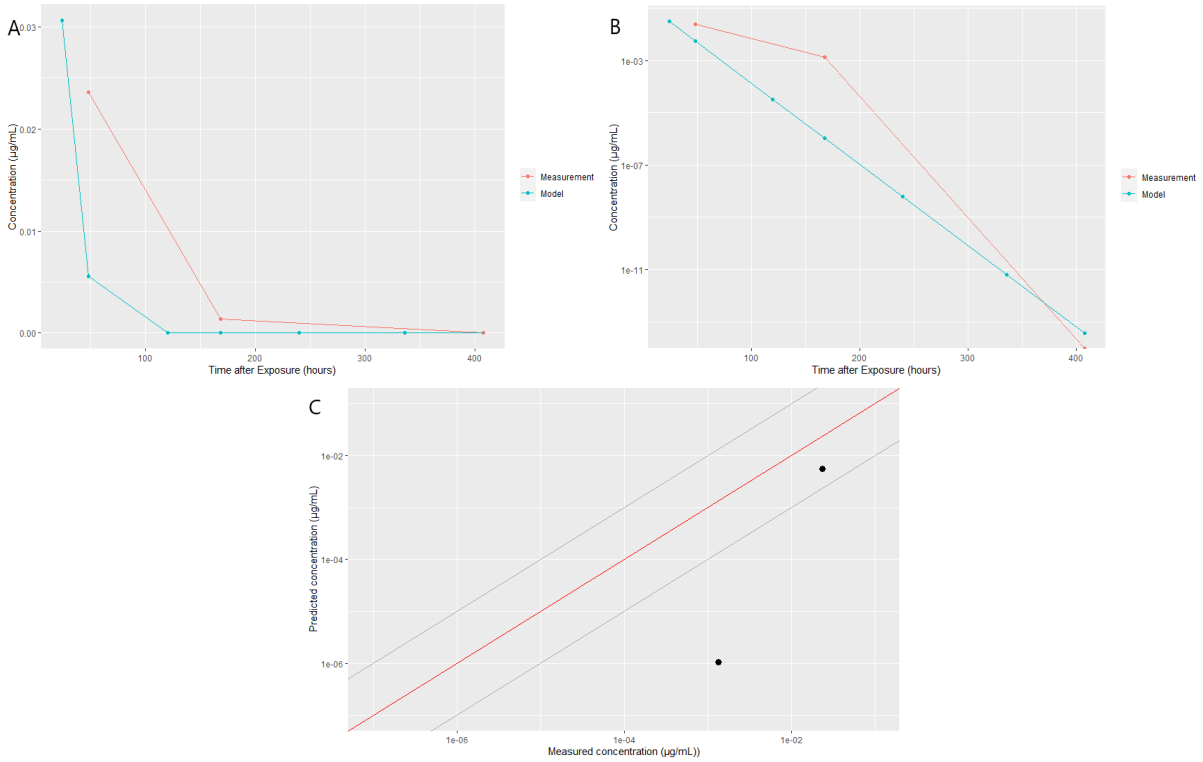

Figure 4.5: Ivermectin in the intestinal mucosa. (A) Ivermectin concentration over time. (B) Ivermectin concentration over time in a semi-logarithmic plot. (C) Predicted concentrations versus measured concentrations for ivermectin in the intestinal mucosa. Both axes are on log-scale. The red line shows the 1:1 line when predicted and measured concentrations match perfectly. The gray lines above and below represent a deviation of factor 10 of the 1:1 line.

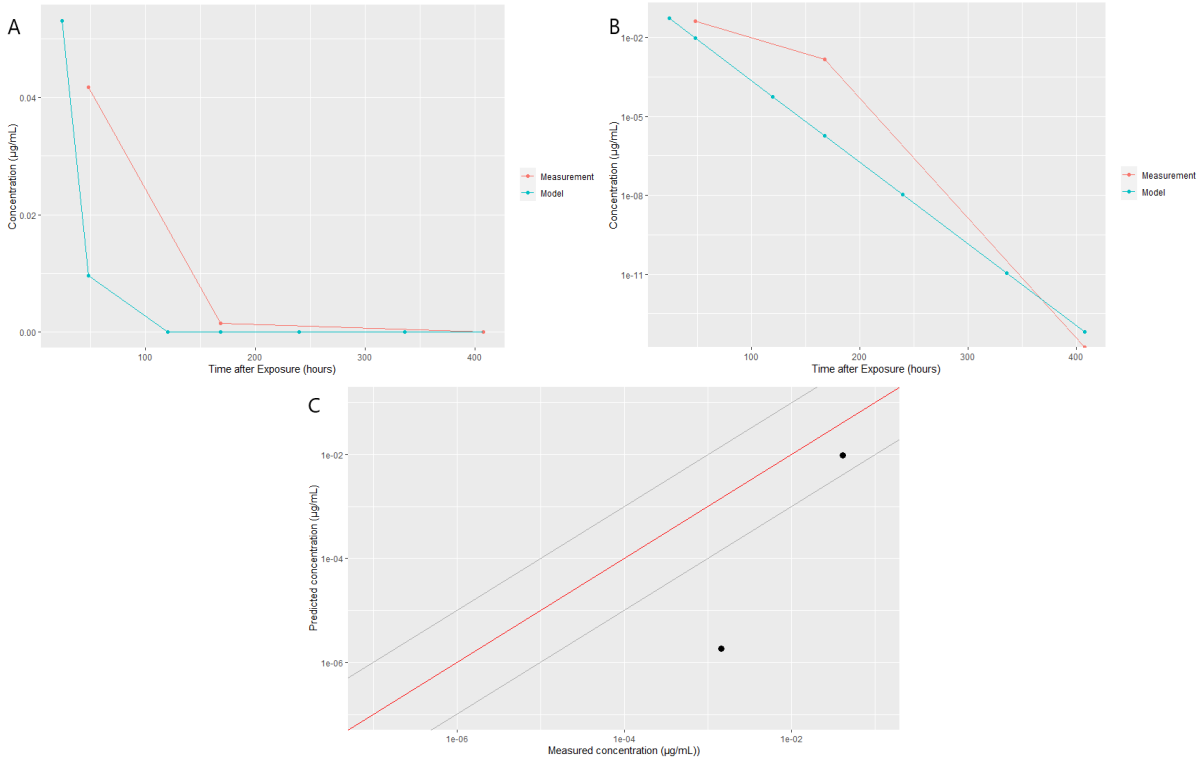

Figure 4.6: Ivermectin in the liver. (A) Ivermectin concentration over time. (B) Ivermectin concentration over time in a semi-logarithmic plot. (C) Predicted concentrations versus measured concentrations for ivermectin in the liver. Both axes are on log-scale. The red line shows the 1:1 line when predicted and measured concentrations match perfectly. The gray lines above and below represent a deviation of factor 10 of the 1:1 line.

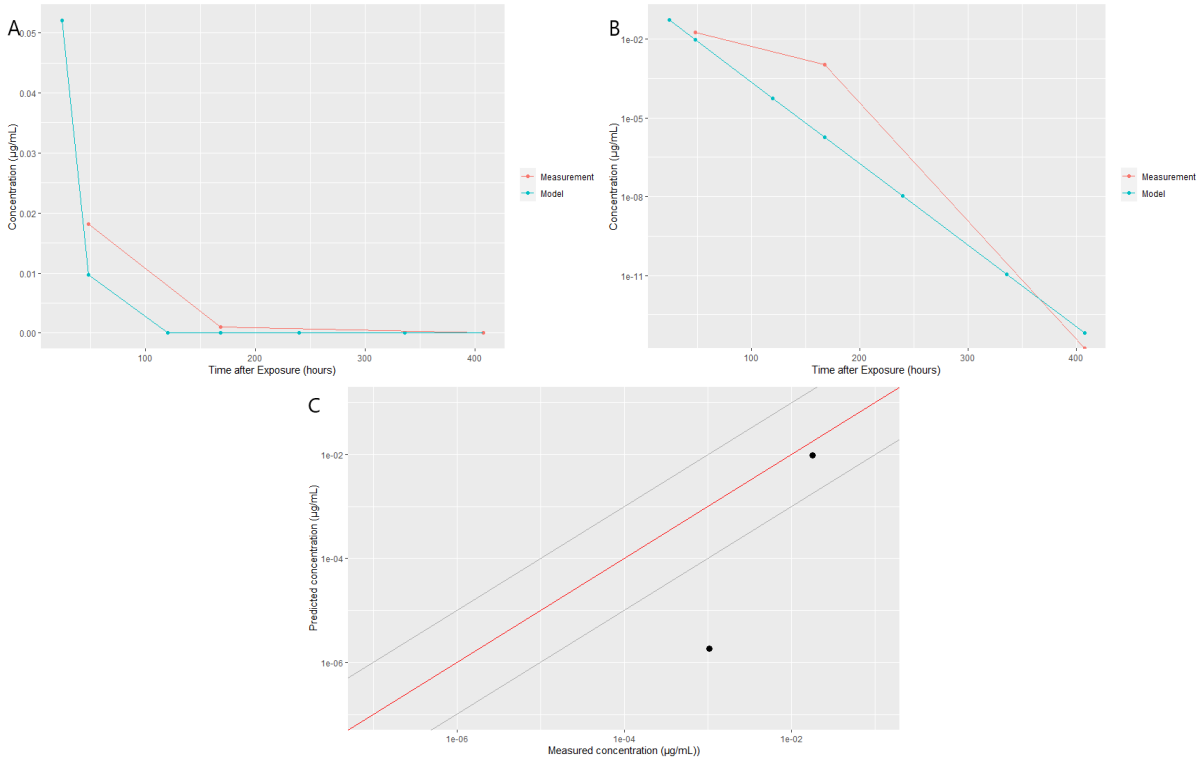

Figure 4.7: Ivermectin in the lungs. (A) Ivermectin concentration over time. (B) Ivermectin concentration over time in a semi-logarithmic plot. (C) Predicted concentrations versus measured concentrations for ivermectin in the lungs. Both axes are on log-scale. The red line shows the 1:1 line when predicted and measured concentrations match perfectly. The gray lines above and below represent a deviation of factor 10 of the 1:1 line.

4.3 Case Study Chloramphenicol

4.3.1 Description of Compound

Chloramphenicol is an antibiotic that can be used against Gram-positive and Gram-negative bacteria (EFSA CONTAM, 2014). It is used against infections in animals and humans. It is a natural product, originally coming from the bacterium *Streptomyces venezuelae*, but is also artificially mass-produced. The chemical structure of chloramphenicol is shown in Figure 4.8.

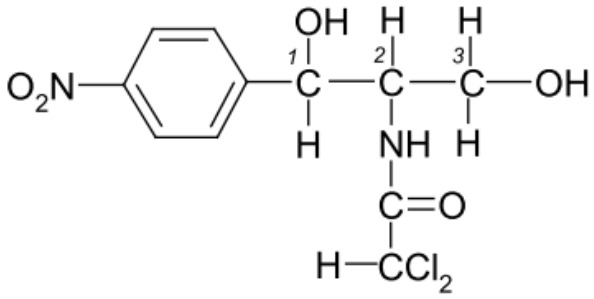

Figure 4.8: Chemical Structure of Chloramphenicol (EFSA CONTAM, 2014).

The use of chloramphenicol was banned from the food production chain in the European Union (EU) in 1994, and is now only allowed in non-food producing animals (EFSA CONTAM, 2014; Hanekamp & Bast, 2015). In other parts of the world however, such as South-East Asia, it is still widely used. The ban by the EU was due to the fact that not enough scientific data were available and therefore no Acceptable Daily Intake (ADI) and Maximum Residu Level (MRL) in food could be established, leading to a zero-tolerance policy.

Etuk and Onyeyili (2005b) show that chloramphenicol is not or incompletely metabolized by the liver. The main route of excretion for this compound is renal clearance. There is also evidence that chloramphenicol is one of few antibiotics that can cross physiological barriers and can therefore enter the brain and cerebrospinal fluid (Etuk & Onyeyili, 2005b).

4.3.2 Description of Validation Study

The goal of the study by Etuk and Onyeyili (2005b) was to compare the distribution of chloramphenicol in tissues between healthy and *Salmonella typhimurium* infected goats, after intravenous treatment. A group of 54 red Sokoto goats of mixed gender were used, with weights ranging from 15.0 to 25 kilograms (mean = 18.3kg). Two groups of 24 goats each were made, one consisting of healthy goats, while the second group was infected with *Salmonella typhimurium*. These goats were given a dose of 25 mg chloramphenicol per kilogram body weight intravenously. Two goats of each group were sacrificed at different time intervals, to collect tissue samples for testing. Ten grams of the following tissues were collected: liver, skeletal muscle, brain, lungs, kidney, spleen and bone marrow. For the validation of this PBK model, the data collected from the group of healthy animals were used.

4.3.3 Results of Model Run

The model simulation of chloramphenicol was done using the data (as described in Chapter 3) for mixed goats, with a 'standardized' body weight of 17.8 kg. Multiple compartments were simulated: liver, kidney, heart, lungs, brain and (skeletal) muscle. In the validation study, spleen and bone marrow were also measured but these compartments are not included in the model and were therefore not simulated.

The case study by Etuk and Onyeyili (2005b) measured chloramphenicol concentrations at 11 time points, namely 0.08, 0.25, 0.50, 1.00, 3.00, 6.00, 12.00, 24.00, 48.00, 120.00 and 240.00 hours. The model gave results for the same time points. The results are shown in Table B.2 in Appendix B.

Figures 4.8 through 4.14 show a comparison between the measured and predicted concentrations for chloramphenicol for the different compartments. Two patterns can be distinguished. In the first pattern, the predicted concentration initially increases and only decreases after a certain time after exposure. This is the case for the brain, heart, liver and lungs. The turning point is between 6 and 12 hours after exposure. For the other two compartments, namely muscle and kidney, the predicted

concentrations decrease from the first data point (at t = 0.08 h) to the last data point (at t = 240 h). Differences between the measured and predicted concentrations range from being similar to the measured concentrations being a factor of 180 larger than predicted.

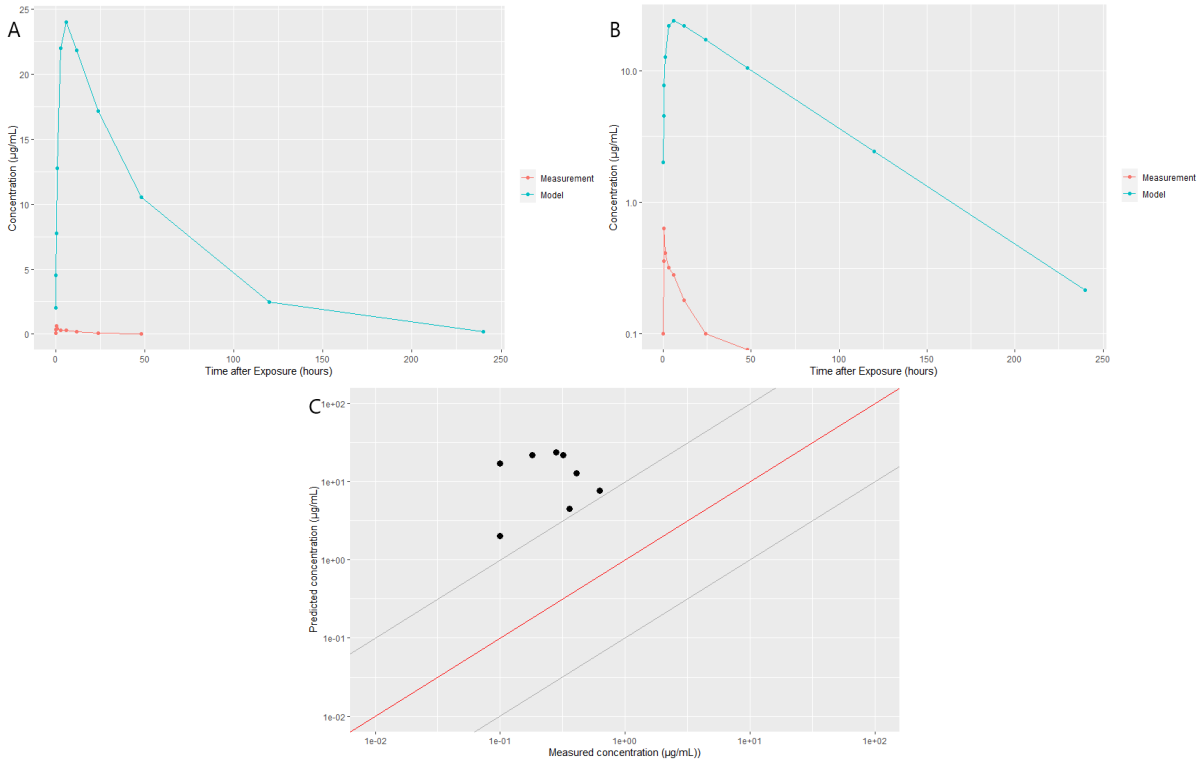

Figure 4.9: Chloramphenicol in the brain. (A) Chloramphenicol concentration over time. (B) Chloramphenicol concentration over time in a semi-logarithmic plot. (C) Predicted concentrations versus measured concentrations for chloramphenicol in the brain. Both axes are on log-scale. The red line shows the 1:1 line when predicted and measured concentrations match perfectly. The gray lines above and below represent a deviation of factor 10 of the 1:1 line.

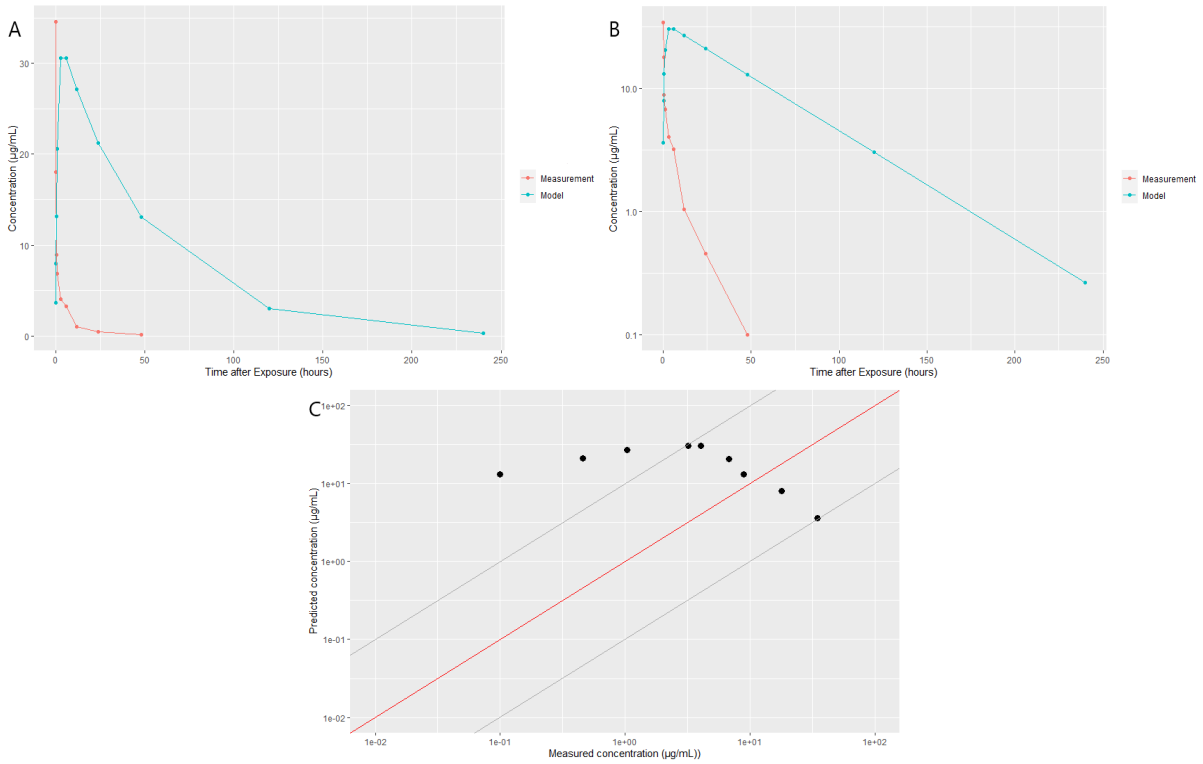

Figure 4.10: Chloramphenicol in the heart. (A) Chloramphenicol concentration over time. (B) Chloramphenicol concentration over time in a semi-logarithmic plot. (C) Predicted concentrations versus measured concentrations for chloramphenicol in the heart. Both axes are on log-scale. The red line shows the 1:1 line when predicted and measured concentrations match perfectly. The gray lines above and below represent a deviation of factor 10 of the 1:1 line.

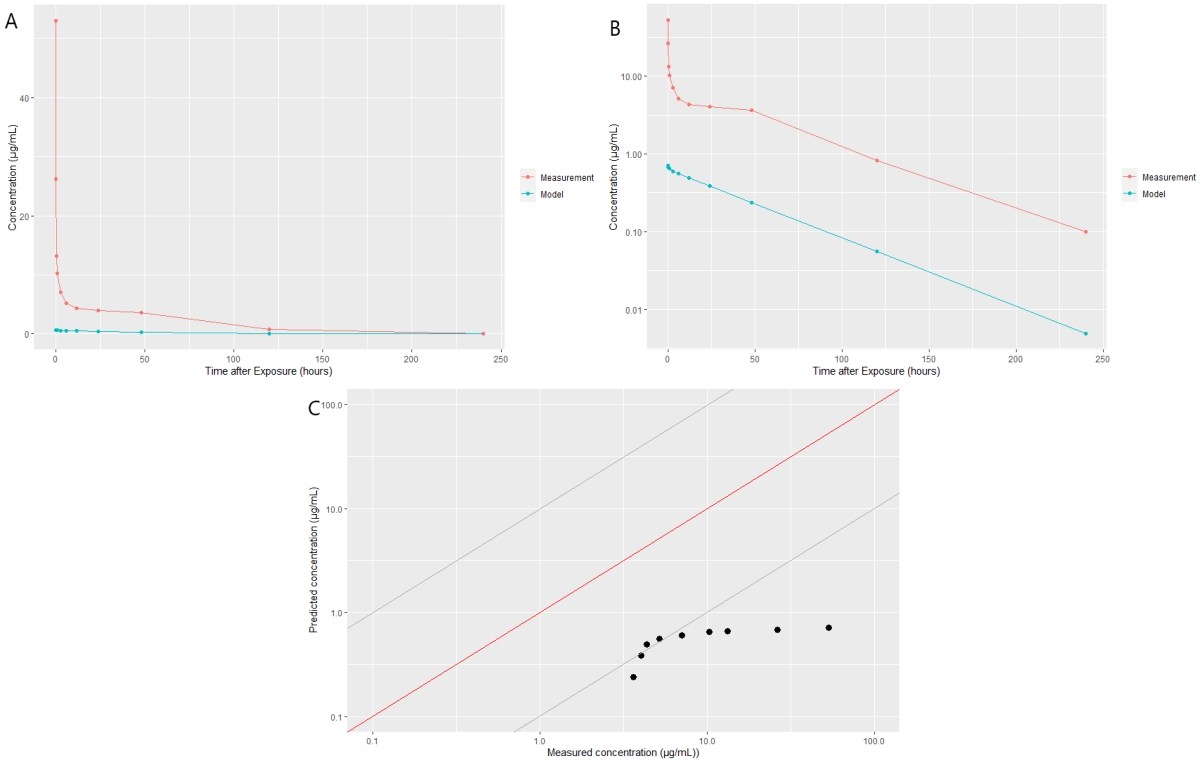

Figure 4.11: Chloramphenicol in the kidney. (A) Chloramphenicol concentration over time. (B) Chloramphenicol concentration over time in a semi-logarithmic plot. (C) Predicted concentrations versus measured concentrations for chloramphenicol in the kidney. Both axes are on log-scale. The red line shows the 1:1 line when predicted and measured concentrations match perfectly. The gray lines above and below represent a deviation of factor 10 of the 1:1 line.

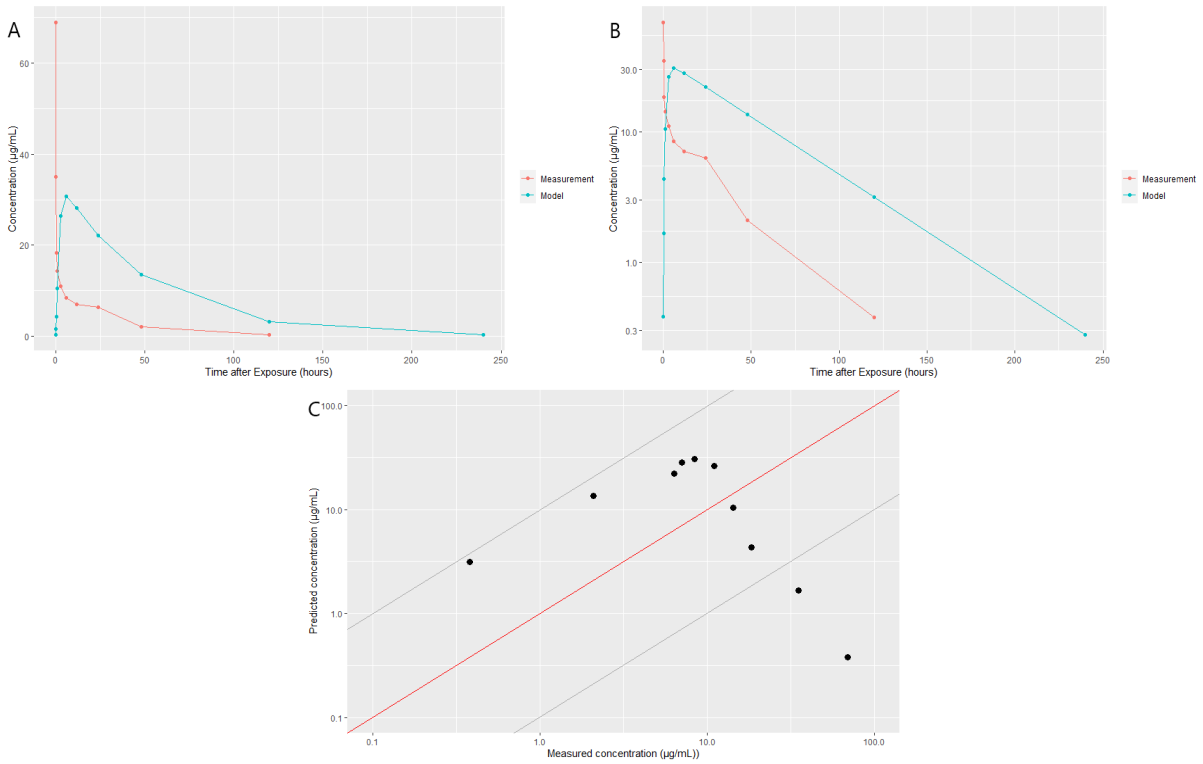

Figure 4.12: Chloramphenicol in the liver. (A) Chloramphenicol concentration over time. (B) Chloramphenicol concentration over time in a semi-logarithmic plot. (C) Predicted concentrations versus measured concentrations for chloramphenicol in the liver. Both axes are on log-scale. The red line shows the 1:1 line when predicted and measured concentrations match perfectly. The gray lines above and below represent a deviation of factor 10 of the 1:1 line.

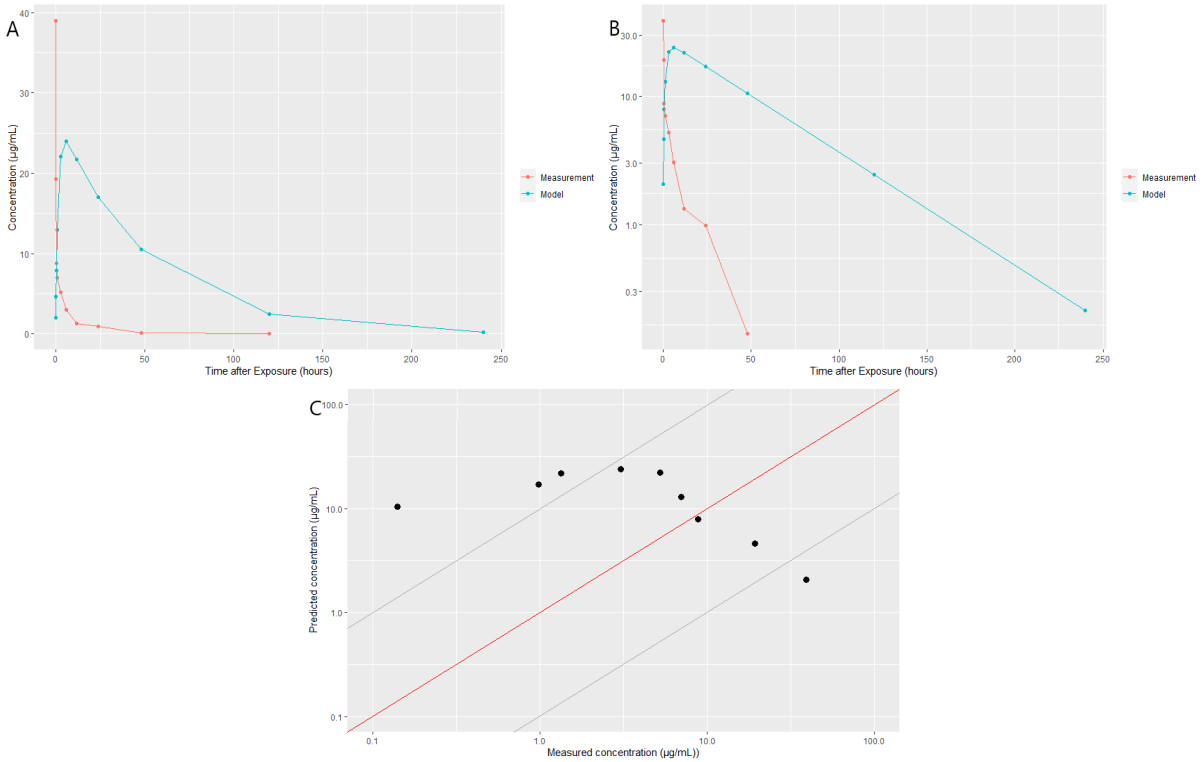

Figure 4.13: Chloramphenicol in the lungs. (A) Chloramphenicol concentration over time. (B) Chloramphenicol concentration over time in a semi-logarithmic plot. (C) Predicted concentrations versus measured concentrations for chloramphenicol in the lungs. Both axes are on log-scale. The red line shows the 1:1 line when predicted and measured concentrations match perfectly. The gray lines above and below represent a deviation of factor 10 of the 1:1 line.

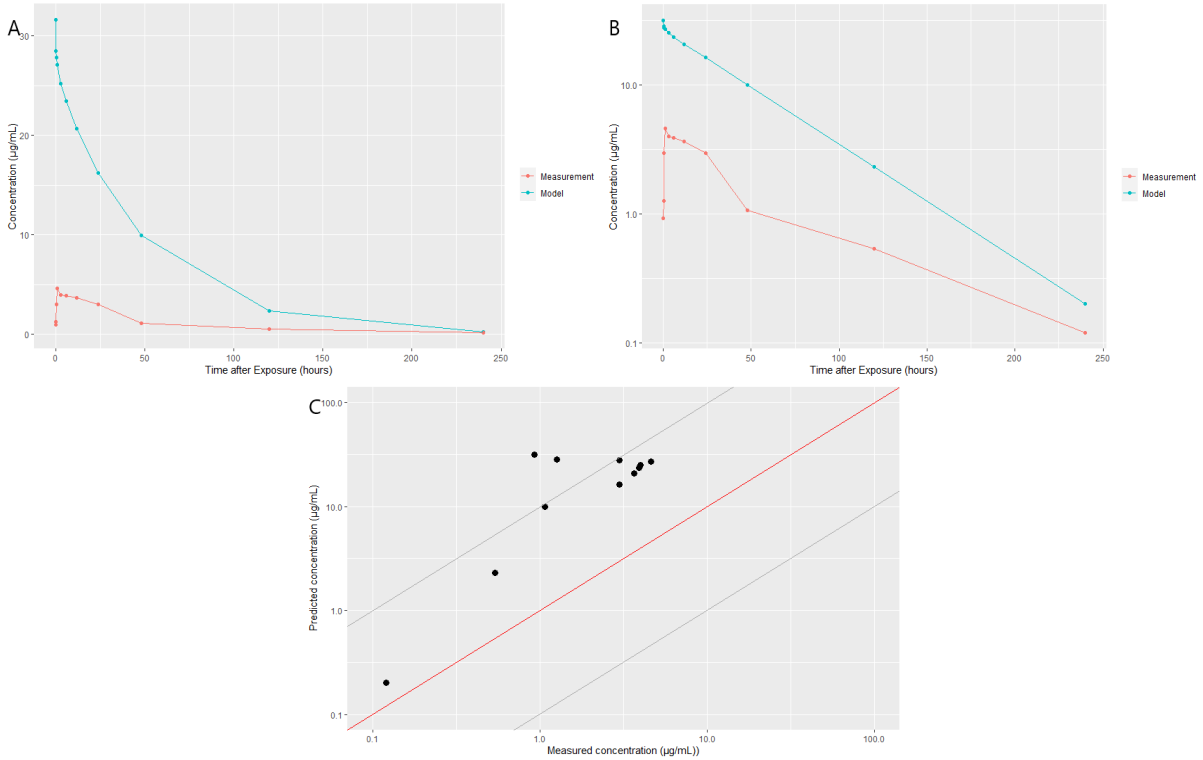

Figure 4.14: Chloramphenicol in the muscle. (A) Chloramphenicol concentration over time. (B) Chloramphenicol concentration over time in a semi-logarithmic plot. (C) Predicted concentrations versus measured concentrations for chloramphenicol in the muscle. Both axes are on log-scale. The red line shows the 1:1 line when predicted and measured concentrations match perfectly. The gray lines above and below represent a deviation of factor 10 of the 1:1 line.

4.4 Case Study Moxifloxacin

4.4.1 Description of Compound

The third compound chosen to use for the validation is moxifloxacin. Moxifloxacin is a fluoroquinolone antibiotic, that, like chloramphenicol, can be used to treat a large range of Gram-positive and Gram-negative bacteria, anaerobes and atypical organisms (Barman Balfour & Wiseman, 1999; Fernández-Varón et al., 2006; Goudah, 2008; Keating & Scott, 2004).

Most common used routes of exposure are oral, intravenous and subcutaneous. The route that is used, strongly impacts the efficiency of the moxafloxacin (Fernández-Varón et al., 2006). Another important factor is the dosage used for treatment (Goudah, 2008). Studies show that there are differences in the pharmacokinetics of moxifloxacin between lactating and non-lactating animals of the same species (Fernández-Varón et al., 2006). Therefore this has to be taken into consideration when dosages are extrapolated between lactating and non-lactating individuals of the same species.

Moxifloxacin is metabolized into two metabolites: M1 (sulpho-compound) and M2 (acyl-glucuronide) (Stass & Kubitza, 1999). The metabolite M1 strongly binds to plasma proteins (90%) and is mainly excreted in the feces. The second metabolite, M2, does not bind to plasma proteins as much (only 5%), and is mainly excreted in the urine. Figure 4.9 shows the metabolism of moxifloxacin. Around 20% of the dose of moxifloxacin is excreted without being metabolized, as the parent compound.

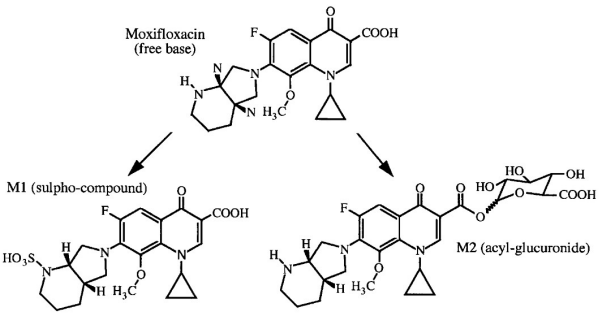

Figure 4.15: Chemical Structure of Moxifloxacin and its metabolites (Stass & Kubitza, 1999).

4.4.2 Description of Validation Study

The aim of the study by Fernández-Varón et al. (2006) was to determine the plasma pharmacokinetics and penetration of moxifloxacin from blood to milk in lactating goats, after it was given intravenously or subcutaneously. Six female goats were used in this study, weighing between 32.1 and 52 kilograms. They were administered a single dosage of 5 mg moxifloxacin per kilogram of body weight. Blood and milk samples were collected at specific time intervals after the drug was given and the concentration of moxifloxacin in these samples was determined using modified high performance liquid chromatography (Fernández-Varón et al., 2006).

4.4.3 Results of Model Run

The model simulation of moxifloxacin was done using the data (as described in Chapter 3) for a female goat, with a 'standardized' body weight of 16.8 kg. Only two compartments were simulated for this model run, namely plasma and milk. This is also the case for the validation study. In the study by Fernández-Varón et al. (2006), the concentration of moxifloxacin in the plasma was measured at 0, 5, 10, 15, 30 and 45 minutes after exposure, and at 1, 1.5, 2, 4, 6, 8, 10, 12, 24, 32, 48 and 72 hours after the drug was administered. The concentration in the milk was measured at 2, 4, 6, 8, 10, 24, 32, 48 and 72 hours after exposure. The udder was emptied at the start of the measurements and at every time point.

Figure 4.16 shows the measured and predicted moxifloxacin concentrations in plasma. The predicted and measured concentrations for plasma are similar until 6 hours after exposure. After 6 hours, the measured concentration decreases much faster than the predicted concentrations. The modeled concentrations remain higher (up to 100 times at t = 12 hours after exposure) than those measured in the study by Fernández-Varón et al. (2006). Figure 4.17 shows a similar trend for the concentration of moxifloxacin in milk over time. For the first points, at t = 2 and t = 4 hours after exposure, the predicted concentrations are 3 - 5 times higher than the measured concentrations. This difference increases to factor 20 at 6 hours after exposure, and continues to increase to the predicted concentration being around 200 times larger than the measured concentration at 32 hours after exposure.

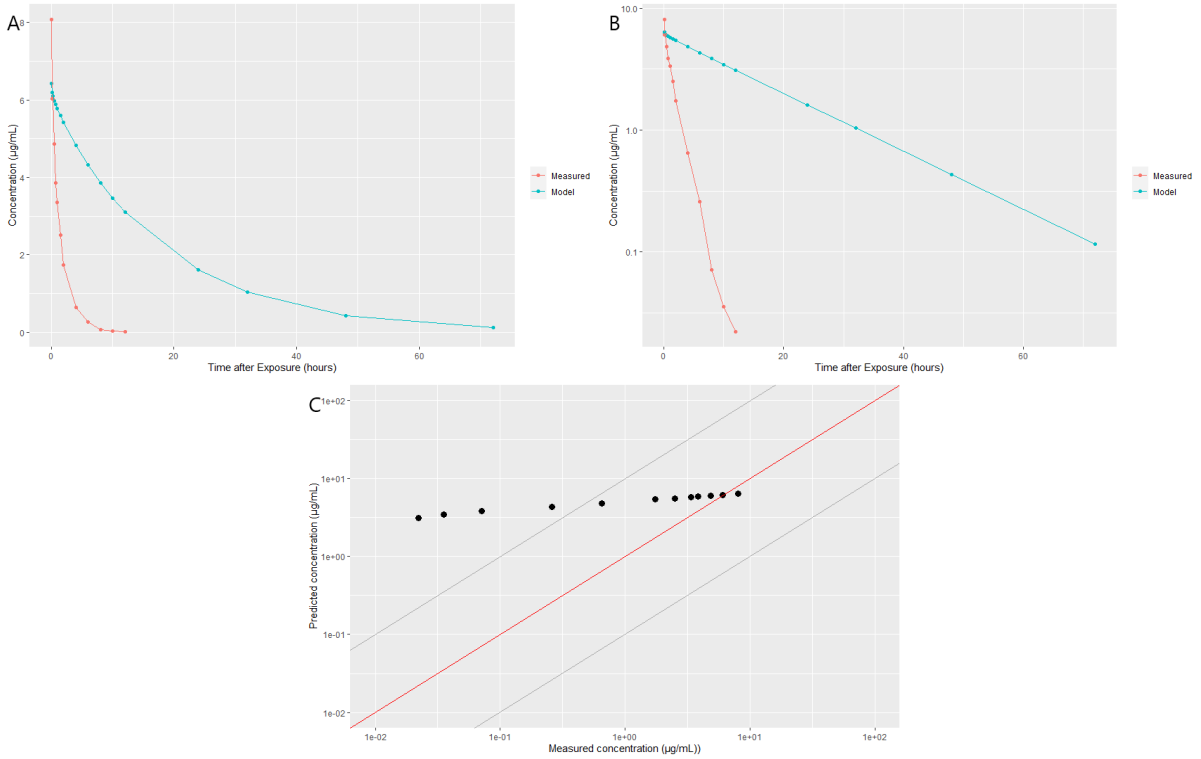

Figure 4.16: Moxifloxacin in the plasma. (A) Moxifloxacin concentration over time. (B) Moxifloxacin concentration over time in a semi-logarithmic plot. (C) Predicted concentrations versus measured concentrations for moxifloxacin in the plasma. Both axes are on log-scale. The red line shows the 1:1 line when predicted and measured concentrations match perfectly. The gray lines above and below represent a deviation of factor 10 of the 1:1 line.

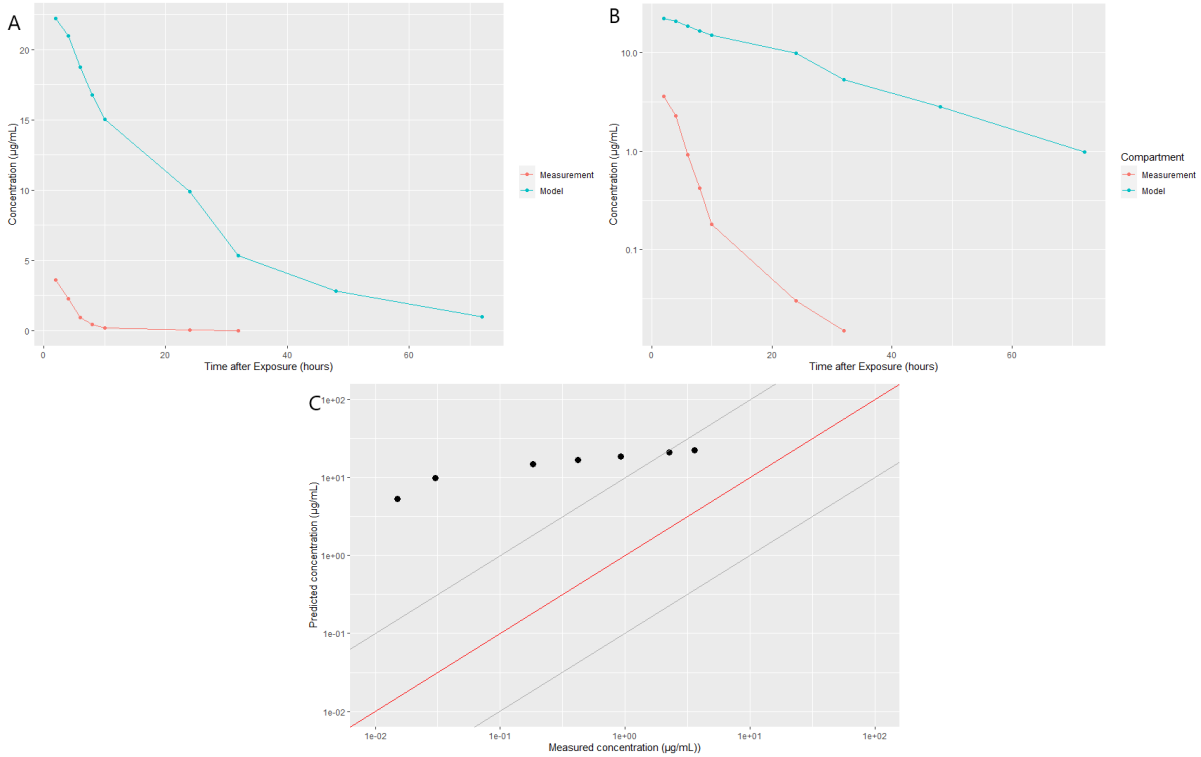

Figure 4.17: Moxifloxacin in the milk. (A) Moxifloxacin concentration over time. (B) Moxifloxacin concentration over time in a semi-logarithmic plot. (C) Predicted concentrations versus measured concentrations for moxifloxacin in the milk. Both axes are on log-scale. The red line shows the 1:1 line when predicted and measured concentrations match perfectly. The gray lines above and below represent a deviation of factor 10 of the 1:1 line.

Chapter 5

Discussion, Conclusions and Recommendations

First the results presented in Chapter 4 are discussed. In Section 5.2 conclusions are drawn based on this discussion. Here, the main research question is also answered. The chapter finalizes with several recommendations.

5.1 Discussion

This section discusses the steps that were taken to adjust the generic PBK model platform (Lautz et al., 2017) to represent the goat. The adjustments, assumptions, parametrization and validation are looked at to ultimately answer the main research question in the conclusion section of this chapter.

5.1.1 Model Parametrization and Implementation

In order to implement the model, values had to be determined for all model input parameters. This was done using multiple literature studies. Finding suitable values was sometimes difficult because of the limited amount of studies done on goats. As explained in Section 3.2, for the physiological parameters where no data was available for goats, values of sheep were used or informed assumptions were made. The general assumption is that sheep and goats are sufficiently similar. However, on specific physiological properties the two species differ. These include the body weight fractions of the carcass, blood, fat, muscle and mammary gland and the fractions of the cerebral, cardiac, intestinal, renal, pulmonary and muscular blood flows. This could influence the described ADME-processes and results of the model (Clewell & Clewell, 2008).

As described in Section 2.2.1, Lautz et al. (2017) assume a blood flow-limited model. This shows that the blood flow through a tissue is an important factor in the accuracy of the model. The differences in blood flow fractions between goats and sheep could therefore result in deviating concentrations predicted by the goat-adjusted model. By adjusting these values to more accurately fit the goat physiology, the results of the model would likely also become more accurate.

Another factor influencing the results is missing data for several parameters, namely f_{bile}, V_{max}, f_{bact} and K_m. Clewell and Clewell (2008) mention that it is difficult to measure these *in vitro* or *in vivo*, leading to this data often being unobtainable. Due to the lack of data, these were set on '0' or as 'Not Available'. Because of this, the metabolism process might not be accurately modeled in the current goat-adjusted model.

Parameters f_{bile} and f_{bact} determine to what extent enterohepatic circulation takes place. Setting these parameters to 0, effectively means that this process is negligible in the current model. However, studies show that enterohepatic circulation does play a role in the metabolizing process of the compounds used in this thesis (De Smet et al., 2012; Duthaler et al., 2020; Tsai et al., 1999). It is unclear how large the impact of this process could be on the results as predicted by the model. However, it is a definite possibility that the unavailability of enterohepatic recycling in the model influenced the results and adding this process would increase the quality of the predicted results.

V_{max} and K_m are parameters that are used to simulate the metabolism process in organs. However, values for these parameters are often lacking. The current model uses (hepatic) clearance as an alternative to

describe the metabolism process. The hepatic metabolism differs significantly between species (Lautz et al., 2017). Using hepatic clearance in the model likely influenced the predicted results for chloramphenicol. Because this compound is not or incompletely metabolized in the liver, hepatic clearance does not accurately describe its metabolism process. This is not the case for ivermectin and moxifloxacin, as these are mostly metabolized in the liver. Therefore, for these compounds hepatic clearance can be used to accurately predict internal concentrations by the PBK model.

5.1.2 Model Validation

The validation studies should give data regarding the tissue distribution of the compound. Especially important were the compound concentrations in blood, liver, urine, and other compartments. There were very few available studies on goats that fit this criterion. The few acquirable compounds limited the opportunity to accurately validate the goat-adjusted PBK model. The values for the toxicokinetic parameters and rates, namely k_{abs}, Cl_{renal} and $Cl_{hepatic}$, were estimated using allometric scaling due to the lack of available goat data. Data from sheep and cattle were used for this allometric scaling. These estimations could be not sufficiently accurate.

The hepatic clearance rates for ivermectin and moxifloxacin were extrapolated using allometric scaling. As hepatic clearance plays an important role in metabolizing these compounds, the allometric scaling should not have been applied. This error could be a cause for the found differences between the predicted and measured concentrations for these compounds.

The results of Chapter 4 show that the current goat-adjusted PBK model can, to a certain extent, accurately predict the distribution of compounds into different compartments in the goat. For each of the compounds looked at, a large part of the predicted concentrations were within factor 10 of the measured concentrations. For ivermectin, 41% of the predictions were within a factor 10 of the measured values. For chloramphenicol, 53% of the predictions were within a factor 10 of the measured values. For moxifloxacin, 55% of the predictions were within a factor 10 of the measured values.

For all modeled compounds however, the results were only partly similar to the measured concentrations. This has to do with specific physicochemical characteristics of the
compounds that are not correctly taken into consideration in the model. The model assumes that the rate of uptake of the compounds are flow-limited. This is not always an accurate assumption, as the uptake of compounds can be impacted by other factors (Clewell & Clewell, 2008). These factors influence biological processes such as storage of the compounds or penetration of the blood-brain or blood-milk barriers. These physicochemical characteristics and biological processes are not explicitly taken into account in the current model, which may explain the divergent results. The effects of these factors are discussed per compound in the following sections.

Ivermectin

In the study by Lespine et al. (2005), the concentration of ivermectin in fat tissue is significantly higher than in the other tissues. This could be explained by storage of ivermectin in fat tissue. Ivermectin has high lipid solubility, which could lead to the compound being stored in fat tissue. It can then slowly be released into the body (Lanusse et al., 1997, Lespine et al., 2005 and Mestorino et al., 2003).

Other studies give similar explanations for the distribution of ivermectin. The study by Begone Ndong et al. (2007) shows sex-dependent differences between the pharmacokinetic values for ivermectin in sheep. The values for female sheep are 68.7% higher than those for male sheep. Their main explanation for this difference, is the difference in fat between male and female sheep. The fat tissue then works as storage for the ivermectin, leading to a longer residence time in the body.

A study by Cerkvenik et al. (2002) looked at the levels of ivermectin in plasma and milk in lactating sheep. They found an increasing ivermectin milk to plasma concentration over time. This was due to the increase in milk fat over time (Cerkvenik et al., 2002). This conclusion was drawn based on the high lipophilicity of ivermectin, influencing its distribution throughout the body and the milk.

The current PBK model does not accurately describe how the adipose tissue retains ivermectin. This could explain the lower predicted ivermectin concentration in fat tissue, when compared to the measured concentration. In addition, the storage in fat tissue leads to a slower release of ivermectin into other parts of the body. This would explain why the measured concentrations in the other compartments decrease at a slower rate than the PBK model predicts. There are two possible reasons for this inaccuracy. The

first is that the fraction of adipose tissue is underestimated. This would mean that there is more adipose tissue and therefore more ivermectin can be stored.

The other possibility is that it takes more time for ivermectin to be released into the blood from the adipose tissue than is described. The current model assumes an instant equilibrium between blood and organ tissue. The high K_{ow} value (1584.89) of ivermectin would lead to a slow release of this compound from adipose tissue into blood and to an underestimation of the concentration over time by the current PBK model. Adjusting the model to more accurately describe this process of slow release, would lead to more fitting results at later exposure phases.

There are multiple administration routes for ivermectin, including orally, subcutaneously and via topical administration (Lespine et al., 2005). Oral administration is possible through tablets or solution (Mestorino et al., 2003). The case study by Lespine et al. (2005) makes use of an ivermectin solution. In the goat-adjusted PBK model, it is not specified whether a solution or tablets are used, which could cause different results.

Mestorino et al. (2003) compared the results of ivermectin given to sheep orally, using tablets and solution. Plasma samples were taken at different intervals, ranging from 0.5 to 20 days after exposure. The study showed an absorption rate (k_{abs}) of 0.001 min^{-1} for administration using an oral solution. The k_{abs} for administration using oral tablets was about half of this at $5.80*10^{-4}$ min^{-1}. The elimination rate constants of the two routes were however similar to each other ($1.33*10^{-4}$ and $1.30*10^{-4}$ for solution and tablets respectively) (Mestorino et al., 2003).

The current goat-adjusted PBK model works with an absorption rate constant (k_{abs}) for ivermectin of 0.002 min^{-1}. This is double the value that Mestorino et al. (2003) found for the oral solution and a factor 4 higher for the oral tablets. If assumed that the results of Lespine et al. (2005) have an absorption rate equal to the one found by Mestorino et al. (2003) (0.001 min^{-1}), the modeled absorption is twice as fast as the validation study. This means that twice the amount of compound is absorbed by the gut tissue from the gut lumen. This leads to higher predicted ivermectin concentrations in the gut and liver, in comparison to the measured concentrations. This does, however, not show in the results, as the predicted concentrations for the liver and intestinal mucosa are in fact lower than the measured concentrations. This means that the higher absorption rate constant is not the crucial factor causing the differences in the results.

Chloramphenicol

For the brain, heart, liver and lungs, the predicted concentrations of chloramphenicol initially increase and start decreasing after t = 6 hours after exposure. This is not the case for the measured concentrations, which immediately decrease (Etuk & Onyeyili, 2005b). This indicates that the modeled absorption rate (0.0889 min^{-1}) is too slow.

Other studies show faster absorption rates. A study by Abdullah and Baggot (1986), shows an absorption rate constant of 0.0954 min^{-1}. Another study by Etuk et al. (2005) gives an absorption rate of 0.110 min^{-1}. A higher absorption rate (k_{abs}) means faster chloramphenicol uptake by the gut. This influences the distribution throughout the body, and therefore leads to higher concentrations in other compartments sooner after exposure starts.

The brain is the only compartment where the predicted concentrations are higher than the measured concentrations at all points in time after exposure. The difference ranges from factor 12 to a factor 171 higher. An explanation could be the transfer of chloramphenicol through the blood-brain barrier (BBB). Criteria for a compound to transfer over the BBB in significant amounts are high lipid solubility and a low molecular weight (< 600 Da) (Banks, 2009; Pardridge, 1995). Chloramphenicol has both these characteristics and therefore can cross the BBB both actively and passively. This is confirmed by multiple literature sources, including Das and Patra (2017) and Moffa and Brook (2015).

The current PBK model however, does not explicitly take this transfer over the blood-brain barrier into account but treats the brain as any other compartment. This could explain the relatively large differences between the predicted and measured concentrations in the brain. If the processes of passive and active transfer over the BBB are more accurately defined in the model, this would limit the amount of compound that transfers over the BBB, leading to lower predicted concentrations. The predicted concentrations would then likely come closer to the measured concentrations.

The high lipid solubility of chloramphenicol could also lead to storage in the liver and adipose tissue. This could explain why the measured concentrations in the liver are much higher in comparison to the other compartments and shows a relatively high concentration after 120 hours after exposure. As is the case for ivermectin, the PBK model does not accurately describe the time needed for the compound to be released from the liver and adipose tissue into the blood. This could explain why the predicted concentrations in the liver do not differ as much from the other compartments, as is the case for the measured concentrations.

Moxifloxacin

After 6 hours of exposure, the predicted moxifloxacin concentrations increase to being a factor 100 to 200 larger than the concentrations measured by Fernández-Varón et al. (2006). As is the case with ivermectin and chloramphenicol, moxifloxacin is also stored in the liver and adipose tissue and released into the blood. This release is slower than the model simulates. This leads to the measured concentrations in the blood and milk to be lower than the predicted concentrations in these compartments.

Multiple studies report that there are differences in the pharmacokinetics of fluoroquinolones, such as moxifloxacin, between lactating and non-lactating individuals of the same species (Cárceles et al., 2007, Cárceles et al., 2009, Fernández-Varón et al., 2006, Soback et al., 1994). The current model does not distinguish between lactating and non-lactating individuals of the same species. This could be an explanation for the increasing differences between the measured and predicted concentrations.

Moxifloxacin penetrates from the blood into the milk and is then excreted from the body through the milk. This explains the higher concentrations in the milk in comparison to the plasma that are found in the model as well as the validation study. Moxifloxacin is an amphoteric compound with multiple pKa values between 6.4 and 9.5. As goat milk has a pH of 6.6 to 6.8, moxifloxacin crosses the blood-milk barrier easily through (passive) diffusion and (active) ion-trapping (Cárceles et al., 2007, Fernández-Varón et al., 2006).

The current PBK model does not explicitly take the blood-milk barrier into consideration. This could be another explanation for the higher predicted concentrations and the increasing differences to the measured moxifloxacin concentrations. Adding a description of the blood-milk barrier into the model, might lead to more accurate results. However, as moxifloxacin easily crosses the blood-milk barrier, it is unclear how much influence adding the transfer processes to the model will have on the differences between the measured and predicted concentrations in the milk.

5.2 Conclusions and Recommendations

The aim of this study was to adjust the existing PBK model platform developed by Lautz et al. (2017), to accurately describe the internal dose of compounds in the goat. In addition, the model should be generic: usable for multiple compartments and compounds. This led to the main research question: Can the available PBK model structure for farm animals as developed by Lautz et al. (2017) be adapted and parameterized to result in a PBK model for goats that can be used to accurately describe the internal dose of compounds in these animals? In conclusion, the current PBK model accurately (within a factor of 10) predicts concentrations in the early exposure phases. This is however, not the case for all compounds and specific biological processes. At later exposure phases, the model becomes inaccurate, for example due to delayed excretion of compounds.

The main reason for this is the lack of available data on goats. For 17 out of 33 of the physiological parameters, values of sheep were used for one or multiple of the gender categories. Missing toxicokinetic parameters, such as absorption rate constants and clearance rates, were calculated from sheep and cattle data, using allometric scaling. In addition, for several parameters, data were completely lacking. Because of this lack of suitable parameter values in existing literature, the results of the validation of the goat-adjusted PBK model in its current form are disappointing. Some values, such as V_{max} and k_m, are currently completely missing, making an accurate description of the metabolism process impossible. This is also the case for the other species this model was developed for, such as cattle, sheep and chicken. Hepatic clearance is used as an alternative for this process in the current model. This choice could lead to inaccurate results by the current model.

In addition to the missing parameter values, the lack of sufficient validation studies leads to difficulty answering the research question. The reason for this, is that there are too few studies showing the tissue

distribution of compounds in goats and therefore cannot be used to determine whether the predictions are accurate. The available studies showed another point, namely that several biological processes, such as the transfer of compounds over the blood-brain and blood-milk barriers and their storage in fat tissue, are not taken into account in the current PBK model. This leads to an inaccurate description of concentrations over time in several tissues.

Overall, it is recommended to decrease the knowledge gaps and adjust the model to more accurately fit biological processes. Research to define values for parameters related to the metabolism process is necessary in order to be able to describe this process accurately in the model. Additionally, more knowledge is needed to adjust the model to fit other biological processes, such as the transfer of compounds over the blood-brain barrier, blood-milk barrier and the storage of chemicals in (adipose) tissue. Differences between the genders should also be taken into account. These processes are recommended to be added into the current model as well. Finally, more experimental data is necessary to validate the PBK model. If these knowledge gaps are decreased and the model is accurately adjusted, the use of PBK models can be greatly increased in risk assessment. This can lead to a decrease in animals needed for testing and therefore overall animal welfare.

Bibliography

Abdullah, A. S., & Baggot, J. D. (1986). Effect of short term starvation on disposition kinetics of chloramphenicol in goats. *Research in Veterinary Science*, *40*(3), 382–385. doi:10.1016/s0034-5288(18)30555-1

Banks, W. A. (2009). Characteristics of compounds that cross the blood-brain barrier. *BMC Neurology*, *9(Suppl I)*(S3). doi:10.1186/1471-2377-9-S1-S3

Barman Balfour, J. A., & Wiseman, L. R. (1999). Moxifloxacin. *Drugs*, *57*(3), 363–373.

Barnes, R. J., Comline, R. S., & Dobson, A. (1983). Changes in the Blood Flow To the Digestive Organs of Sheep Induced By Feeding. *Quarterly Journal of Experimental Physiology*, *68*(1), 77–88. doi:10.1113/expphysiol.1983.sp002704

Barton, H. A., Chiu, W. A., Woodrow Setzer, R., Andersen, M. E., Bailer, A. J., Bois, F. Y., ... Tan, Y. M. (2007). Characterizing uncertainty and variability in physiologically based pharmacokinetic models: State of the science and needs for research and implementation. *Toxicological Sciences*, *99*(2), 395–402. doi:10.1093/toxsci/kfm100

Bengone Ndong, T., Kane, Y., Diouf, E., & Alvinerie, M. (2007). Ivermectin in senegalese peulh sheep: Influence of sex on plasma disposition. *Veterinary Research Communications*, *31*, 739–747. doi:10.1007/s11259-007-3522-6

Bueters, T., Juric, S., Sohlenius-Sternbeck, A. K., Hu, Y., & Bylund, J. (2013). Rat poorly predicts the combined non-absorbed and presystemically metabolized fractions in the human. *Xenobiotica*, *43*(7), 607–616. doi:10.3109/00498254.2012.752117

Burrin, D. G., Ferrell, C. L., Britton, R. A., & Bauer, M. (1990). Level of nutrition and visceral organ size and metabolic activity in sheep. *British Journal of Nutrition*, *64*(2), 439–448. doi:10.1079/bjn19900044

Campbell, W. C. (1985). Ivermectin: An update. *Parasitology Today*, *1*(1), 10–16. doi:10.1016/0169-4758(85)90100-0

Cárceles, C. M., Escudero, E., Fernández-Varón, E., & Marín, P. (2009). Pharmacokinetics after intravenous, intramuscular and subcutaneous administration of moxifloxacin in sheep. *Veterinary Journal*, *180*(3), 343–347. doi:10.1016/j.tvjl.2007.11.025

Cárceles, C. M., Villamayor, L., Escudero, E., Marín, P., & Fernández-Varón, E. (2007). Pharmacokinetics and milk penetration of moxifloxacin after intramuscular administration to lactating goats. *Veterinary Journal*, *173*(2), 452–455. doi:10.1016/j.tvjl.2005.11.003

Cerkvenik, V., Grabnar, I., Skubic, V., Doganoc, D. Z., Beek, W. M., Keukens, H. J., ... Pogačnik, M. (2002). Ivermectin pharmacokinetics in lactating sheep. *Veterinary Parasitology*, *104*(2), 175–185. doi:10.1016/S0304-4017(01)00612-4

Chiu, W. A., Barton, H. A., Dewoskin, R. S., Schlosser, P., Thompson, C. M., Sonawane, B., ... Krishnan, K. (2007). Evaluation of physiologically based pharmacokinetic models for use in risk assessment. *Journal of Applied Toxicology*, *27*, 218–237. doi:10.1002/jat.1225

Clark, L. H., Setzer, R. W., & Barton, H. A. (2004). Framework for evaluation of physiologically-based pharmacokinetic models for use in safety or risk assessment. *Risk Analysis*, *24*(6), 1697–1717. doi:10.1111/j.0272-4332.2004.00561.x

Clewell, R. A., & Clewell, H. J. (2008). Development and specification of physiologically based pharmacokinetic models for use in risk assessment. *Regulatory Toxicology and Pharmacology*, *50*(1), 129–143. doi:10.1016/j.yrtph.2007.10.012

Das, B., & Patra, S. (2017). Antimicrobials: Meeting the Challenges of Antibiotic Resistance Through Nanotechnology. In A. Ficai & A. M. Grumezescu (Eds.), *Nanostructures for antimicrobial therapy: A volume in micro and nano technologies* (1st ed., Chap. 1, pp. 1–22). Elsevier.

De Smet, J., Colin, P., De Paepe, P., Ruige, J., Batens, H., Van Nieuwenhove, Y., ... Boussery, K. (2012). Oral bioavailability of moxifloxacin after Roux-en-Y gastric bypass surgery. *Journal of Antimicrobial Chemotherapy*, *67*(1), 226–229. doi:10.1093/jac/dkr436

Di Giantomasso, D., Morimatsu, H., May, C. N., & Bellomo, R. (2004). Increasing Renal Blood Flow. *Chest*, *125*(6), 2260–2267. doi:10.1378/chest.125.6.2260

Duthaler, U., Leisegang, R., Karlsson, M. O., Krähenbühl, S., & Hammann, F. (2020). The effect of food on the pharmacokinetics of oral ivermectin. *The Journal of antimicrobial chemotherapy*, *75*(2), 438–440. doi:10.1093/jac/dkz466

EFSA. (2014). Modern methodologies and tools for human hazard assessment of chemicals. *EFSA Journal*, *12*(4). doi:10.2903/j.efsa.2014.3638

EFSA. (2016). EFSA Strategy 2020: Trusted science for safe food. Protecting consumers' health with independent scientific advice on the food chain, 1–32. doi:10.2805/397609

EFSA CONTAM (European Food Safety Authority Panel on Contaminants in the Food Chain). (2014). Scientific Opinion on Chloramphenicol in food and feed. *EFSA Journal*, *12*(11), 3907. doi:10.2903/j.efsa.2014.3907

Etuk, E., & Onyeyili, P. (2005a). Pharmacokinetics of Chloramphenicol in Healthy and Water-deprived Goats. *International Journal of Pharmacology*, *1*(3), 244–248.

Etuk, E., & Onyeyili, P. (2005b). The Comparative Study of the Tissue Kinetics of Chloramphenicol in Healthy and Salmonella Infected Goats. *Pakistan Journal of Biological Sciences*, *8*(3), 369–373.

Etuk, E., Onyeyili, P., & Muhammed, B. (2005). Pharmacokinetics of Chloramphenicol Following Intravenous and Intramuscular Administration of the Drug to Healthy Sokoto Red Goats. *2International Journal of Pharmacology*, *1*(3), 239–243.

EU. (2018). Agriculture statistics at regional level. Retrieved February 15, 2019, from https://ec.europa.eu/eurostat/statistics-explained/index.php?title=Agriculture%7B%5C_%7Dstatistics%7B%5C_%7Dat%7B%5C_%7Dregional%7B%5C_%7Dlevel%7B%5C#%7DAnimals

Fernández-Varón, E., Villamayor, L., Escudero, E., Espuny, A., & Cárceles, C. M. (2006). Pharmacokinetics and milk penetration of moxifloxacin after intravenous and subcutaneous administration to lactating goats. *Veterinary Journal*, *172*(2), 302–307. doi:10.1016/j.tvjl.2005.04.017

Goudah, A. (2008). Disposition kinetics of moxifloxacin in lactating ewes. *The Veterinary Journal*, *178*, 280–285. doi:10.1016/j.tvjl.2007.08.007

Gregory, N. G., Christopherson, R. J., & Lister, D. (1986). Adipose tissue capillary blood flow in relation to fatness in sheep. *Research in veterinary science*, *40*(3), 352–356. doi:10.1016/s0034-5288(18)30549-6

Grimes, J. M., Buss, L. A., & Brace, R. A. (1987). Blood volume restitution after hemorrhage in adult sheep. *American Journal of Physiology - Regulatory Integrative and Comparative Physiology*, *253*(4). doi:10.1152/ajpregu.1987.253.4.r541

Hales, J. R. S. (1973). Effects of exposure to hot environments on total and regional blood flow in the brain and spinal cord of the sheep. *Pflügers Archiv European Journal of Physiology*, *344*(4), 327–337. doi:10.1007/BF00592785

Hales, J. R., & Fawcett, A. A. (1993). Wool production and blood supply to skin and other tissues in sheep. *Journal of animal science*, *71*(2), 492–498. doi:10.2527/1993.712492x

Hanekamp, J. C., & Bast, A. (2015). Antibiotics exposure and health risks: Chloramphenicol. *Environmental Toxicology and Pharmacology*, *39*(1), 213–220. doi:10.1016/j.etap.2014.11.016

Huang, Q., Gehring, R., Tell, L. A., Li, M., & Riviere, J. E. (2015). Interspecies allometric meta-analysis of the comparative pharmacokinetics of 85 drugs across veterinary and laboratory animal species. *Journal of Veterinary Pharmacology and Therapeutics*, *38*(3), 214–226. doi:10.1111/jvp.12174

Keating, G. M., & Scott, L. J. (2004). Moxifloxacin A Review of its Use in the Management of Bacterial Infections. *Drugs*, *64*(20), 2347–2377.

Kisauzi, D. N., & Leek, B. F. (1991). The effects of experimentally induced fever on the estimated blood flow to and oxygen utilization by the liver and the viscera drained by the portal vein in sheep. *Veterinary Research Communications*, *15*(2), 95–105. doi:10.1007/BF00405141

Lanusse, C., Lifschitz, A., Virkel, G., Alvarez, L., Sánchez, S., Sutra, J. F., ... Alvinerie, M. (1997). Comparative plasma disposition kinetics of ivermectin, moxidectin and doramectin in cattle. *Journal of Veterinary Pharmacology and Therapeutics*, *20*(2), 91–99. doi:10.1046/j.1365-2885.1997.00825.x

Lautz, L., Oldenkamp, R., & Ragas, A. (2017). Final report on the data collection of biological, physiological and toxicological variables to calibrate and develop "generic" TK tools for animal risk assessment of single chemicals. Nijmegen: Radboud University.

Leavens, T., Tell, L., Clothier, K., Grifftih, R., Baynes, R., & Riviere, J. (2011). Development of a physiologically based pharmacokinetic model to predict tulathromycin distribution in goats. *Journal of Veterinary Pharmacology and Therapeutics*, *35*, 121–131. doi:10.1111/j.1365-2885.2011.01304.x.Development

Lespine, A., Alvinerie, M., Sutra, J. F., Pors, I., & Chartier, C. (2005). Influence of the route of administration on efficacy and tissue distribution of ivermectin in goat. *Veterinary Parasitology*, *128*(3-4), 251–260. doi:10.1016/j.vetpar.2004.11.028

Liebig, M., Fernandez, Á. A., Blübaum-Gronau, E., Boxall, A., Brinke, M., Carbonell, G., ... Duisy, K. (2010). Environmental risk assessment of ivermectin: A case study. *Integrated Environmental Assessment and Management*, *6*(SUPPL. 1), 567–587. doi:10.1002/ieam.96

Lin, Z., Gehring, R., Mochel, J. P., Lavé, T., & Riviere, J. E. (2016). Mathematical modeling and simulation in animal health - Part II: principles, methods, applications, and value of physiologically based pharmacokinetic modeling in veterinary medicine and food safety assessment. *Journal of Veterinary Pharmacology and Therapeutics*, *39*(5), 421–438. doi:10.1111/jvp.12311

Linzell, J. (1960). Mammary-gland blood flow and oxygen, glucose and volatile fatty acid uptake in the conscious goat. *Journal of Physiology*, *153*, 492–509.

Mahgoub, O. (1997). Meat production from the Omani Dhofari goat . 1 . Live-weight growth and body composition. *International Journal of Animal Sciences*, *12*, 25–30.

Mahgoub, O. [O.], & Lodge, G. A. (1996). Growth and body composition in meat production of Omani Batina goats. *Small Ruminant Research*, *19*(3), 233–246. doi:10.1016/0921-4488(95)00762-8

Mahgoub, O. [O.], & Lodge, G. A. (1998). A comparative study on growth, body composition and carcass tissue distribution in Omani sheep and goats. *Journal of Agricultural Science*, *131*(3), 329–339. doi:10.1017/S0021859698005887

Mahgoub, O. [O.], & Lu, C. D. (1998). Growth, body composition and carcass tissue distribution in goats of large and small sizes. *Small Ruminant Research*, *27*(3), 267–278. doi:10.1016/s0921-4488(97)00055-2

Melsom, M. N., Flatebø, T., Kramer-Johansen, J., Aulie, A., Sjaastad, V., Iversen, P. O., & Nicolaysen, G. (1995). Both gravity and non-gravity dependent factors determine regional blood flow within the goat lung. *Acta Physiologica Scandinavica*, *153*(4), 343–353. doi:10.1111/j.1748-1716.1995.tb09872.x

Mestorino, N., Turic, E., Pesoa, J., Echeverría, J., & Errecalde, J. O. (2003). Pharmacokinetics in plasma of ivermectin after its oral (solution and tablets) administration to sheep. *Journal of Veterinary Pharmacology and Therapeutics*, *26*(4), 307–309. doi:10.1046/j.1365-2885.2003.00485.x

Moffa, M., & Brook, I. (2015). Tetracyclines, Glycylcyclines, and Chloramphenicol. In J. E. Bennet, R. Dolin, & M. J. Blaser (Eds.), *Mandell, douglas, and bennett's principles and practice of infectious diseases* (8th ed., Chap. 26, pp. 322–338). Philadelphia, United States: Saunders.

National Center for Biotechnology Information (NCBI). PubChem Database. (n.d.). Moxifloxacin, CID=152946. Retrieved January 15, 2020, from https://pubchem.ncbi.nlm.nih.gov/compound/Moxifloxacin

Ngwa, A. T., Dawson, L. J., Puchala, R., Detweiler, G. D., Merkel, R. C., Wang, Z., ... Goetsch, A. L. (2009). Effects of breed and diet on growth and body composition of crossbred Boer and Spanish wether goats. *Journal of Animal Science*, *87*, 2913–2923. doi:10.2527/jas.2009-1835

Norberg, Å., Brauer, K. I., Prough, D. S., Gabrielsson, J., Hahn, R. G., Uchida, T., ... Svensén, C. H. (2005). Volume turnover kinetics of fluid shifts after hemorrhage, fluid infusion, and the combination of hemorrhage and fluid infusion in sheep. *Anesthesiology*, *102*(5), 985–994. doi:10.1097/00000542-200505000-00018

Paini, A., Leonard, J. A., Joossens, E., Bessems, J. G., Desalegn, A., Dorne, J. L., ... Tan, Y. M. (2019). Next generation physiologically based kinetic (NG-PBK) models in support of regulatory decision making. *Computational Toxicology*, *9*, 61–72. doi:10.1016/j.comtox.2018.11.002

Pardridge, W. M. (1995). Transport of small molecules through the blood-brain barrier: biology and methodology. *Advanced Drug Delivery Reviews*, *15*(1-3), 5–36. doi:10.1016/0169-409X(95)00003-P

Pelligrino, D. A., Miletich, D. J., Hoffmann, W. E., & Albrecht, R. F. (1984). Nitrous Oxide Markedly Increases Cerebral Cortical Metabolic Rate and Blood Flow in the Goat. *Anesthesiology*, *60*, 405–412.

Peris, S., Caja, G., & Such, X. (1999). Relationships between udder and milking traits in Murciano-Granadina dairy goats. *Small Ruminant Research*, *33*, 171–179. doi:10.1016/S0921-4488(99)00017-6

Ragas, A. M., & Huijbregts, M. A. (1998). Evaluating the coherence between environmental quality objectives and the acceptable or tolerable daily intake. *Regulatory Toxicology and Pharmacology*, *27*(3), 251–264. doi:10.1006/rtph.1998.1212

Soback, S., Gips, M., Bialer, M., & Bor, A. (1994). Effect of lactation on single-dose pharmacokinetics of norfloxacin nicotinate in ewes. *Antimicrobial Agents and Chemotherapy*, *38*(10), 2336–2339. doi:10.1128/AAC.38.10.2336

Stass, H., & Kubitza, D. (1999). Pharmacokinetics and elimination of moxifloxacin after oral and intravenous administration in man. *Journal of Antimicrobial Chemotherapy*, *43*(Suppl. B), 83–90.

Talke, P. O., Traber, D. L., Richardson, C. A., Harper, D. D., & Traber, L. D. (2000). The effect of $\alpha 2$ agonist-induced sedation and its reversal with an antagonist on organ blood flow in sheep. *Anesthesia and Analgesia*, *90*(5), 1060–1066. doi:10.1097/00000539-200005000-00011

Tsai, T. H., Shum, A. Y., & Chen, C. F. (1999). Enterohepatic circulation of chloramphenicol and its glucuronide in the rat by microdialysis using a hepato-duodenal shunt. *Life Sciences*, *66*(4), 363–370. doi:10.1016/S0024-3205(99)00598-6

Ullman, J., Eriksson, S., & Rundgren, M. (2001). Effects of losartan, prazosin and a vasopressin V1-receptor antagonist on renal and femoral blood flow in conscious sheep. *Acta Physiologica Scandinavica*, *171*(1), 99–104. doi:10.1046/j.1365-201X.2001.00780.x

WHO. (2009). Principles and Methods for the Risk Assessment of Chemicals in Food. Chapter 1. Introduction. *Environmental Health Criteria 240*, 1–13.

WHO. (2010). *Characterization and Application of Physiologically Based Pharmacokinetic Models*. doi:10.1109/ICASSP.2014.6855169

Yoon, M., Campbell, J. L., Andersen, M. E., & Clewell, H. J. (2012). Quantitative in vitro to in vivo extrapolation of cell-based toxicity assay results. *Critical Reviews in Toxicology*, *42*(8), 633–652. doi:10.3109/10408444.2012.692115

Appendix A

Model Code

```
#=====================================#
# probabilistic                       #
# multi-compartment model for         #
# veterinary species                  #
#=====================================#

#load one compartment model code
source('singchemdmdtSary.R')
library('sensitivity')
library('reshape')
library('ggplot2')

#define your working directions


#install libraries
#install.packages("sensitivity")

#load libraries
#library('sensitivity')


#Loading physiology data
fBW <- read.csv("data_fBW_animals1.csv",stringsAsFactors = FALSE)       #organ fractions, incl var-distribution parameters
fCO <- read.csv("data_fCO_animals1.csv",stringsAsFactors = FALSE)       #blood flow fractions, incl var-distribution parameters
rates <- read.csv("data_rates_animals1.csv",stringsAsFactors = FALSE)   #physiological rates (not chemical-dependent)
fPC <- read.csv("data_pc_tissue1.csv",stringsAsFactors = FALSE)         #tissue composition, fixed during var-analysis

#Loading TK data
TK <- read.csv("data_TK1.csv",stringsAsFactors=FALSE)                   #toxicokinetic parameters

#Loading physicochemical data
chem <- read.csv("data_chem1.csv", stringsAsFactors = FALSE)       #physicochemical parameters

# Inputs ----
  #Defining the exposure scenario
    species <- "goat_g"              #select the animal
    chemical <- "chloramphenicol"           #select chemical

    regime <- "bolus"               #exposure regime (bolus/continuous)
```

```
  route <- "iv"                  #exposure route (oral/iv)
  E_dose <- 25                 #exposure dose (mg/kgbw)
  E_start <- 0                   #start of exposure phase (h)
  E_end <- 250                 #end of exposure phase (h)
  E_int <- 249                   #interval between doses (h); only relevant when regime="bolus" or iv

#Simulation parameters for monte carlo
  A_type <- "VA"                 #type of probabilistic analysis ("SA" or "VA"), for individuals skip this
  chem_fix <- TRUE               #keep it TRUE
  n_sim  <- 1000                 #number of iterations
  n_boot <- 1000                 #number of boostrap iterations (for SA)

#define output parameters and time
  n_out  <- 7                    #number of compartments to output (blood, liver, kidney, etc.)
  t_start <- 0                   #start of simulation (h)
  t_end <- 240                 #end of simulation (h)
  #all time points for analysis (h), only relevant when chem_fix=TRUE
  t_A <- c(0.08, 0.25, 0.5, 1, 3, 6, 12, 24, 48, 120, 240)
  #t_A <- c(seq(0.025,0.225,by=0.025),seq(0.25,24,by=0.25))

#=============================================================================
#Setup single animal simulation -----

  Names_fix <- c("BW",
                 paste("fBW",colnames(fBW[2+3*c(1:19)]),sep="_"),
                 "CO",
                 paste("fCO",colnames(fCO[2+3*c(1:19)]),sep="_"),
                 colnames(rates[2+3*c(0:4)]),
                 colnames(fPC[2:57]),
                 "nl","pl","pr","w",
                 colnames(TK[3:8]),
                 colnames(chem[2:5]))
  NP_fix <- length(Names_fix) #number of fixed parameters

  fix_in <- cbind(fBW[fBW$species==species,"BW"],
                  fBW[fBW$species==species,colnames(fBW)%in%substr(Names_fix[grep('fBW',Names_fix)],
                                                   start=5,stop=nchar(Names_fix[grep('fBW',Names_fix)]))],
                  fCO[fCO$species==species,"CO"],
                  fCO[fCO$species==species,colnames(fCO)%in%substr(Names_fix[grep('fCO',Names_fix)],
                                                   start=5,stop=nchar(Names_fix[grep('fCO',Names_fix)]))],
```

```
                    rates[rates$species==species,colnames(rates)%in%Names_fix],
                    fPC[fPC$species==species,colnames(fPC)%in%Names_fix],
                    data.frame(nl=1,pl=1,pr=1,w=1),
                    TK[TK$species==species&TK$chemical==chemical,colnames(TK)%in%Names_fix],
                    chem[chem$chemical==chemical,colnames(chem)%in%Names_fix])
  colnames(fix_in) <- Names_fix

  par_in <- fix_in

#=============================================================================
#Set up probabilistic simulations-----
  if (chem_fix & A_type=="SA") {
  #Sensitivity analysis with fixed chem parameters and varying physiology
    #initial list with names of all varying parameters
    Names_var <- c("BW",
                   paste("fBW",colnames(fBW[2+3*c(1:19)]),sep="_"),
                   "CO",
                   paste("fCO",colnames(fCO[2+3*c(1:19)]),sep="_"),
                   colnames(rates[2+3*c(0:4)]),
                   "nl","pl","pr","w")

    #initial list with median values of all varying parameters
    Medians <- cbind(fBW[fBW$species==species,2+3*c(0:19)],
                     fCO[fCO$species==species,2+3*c(0:19)],
                     rates[rates$species==species,2+3*c(0:4)],
                     data.frame(nl=1,pl=1,pr=1,w=1))
    colnames(Medians) <- Names_var
    Names_var_not <- colnames(Medians[which(Medians==0|is.na(Medians))])

    #update distribution parameters for varying parameters
    Medians <- Medians[!(colnames(Medians)%in%Names_var_not)] #exclude all compartments for which median = 0 or NA
    Lower <- Medians - 0.1*Medians
    Upper <- Medians + 0.1*Medians

    Names_var <- colnames(Medians)
    NP_var <- length(Names_var) #number of varying parameters

    #all fixed parameters (including 'varying parameters' that are 0 or NA)
    Names_fix <- c(colnames(TK[3:8]),
                   colnames(chem[2:5]),
```

```
                colnames(fPC[2:57]),
                Names_var_not)
  NP_fix <- length(Names_fix) #number of fixed parameters

  fix_in <- cbind(TK[TK$species==species&TK$chemical==chemical,colnames(TK)%in%Names_fix],
                  chem[chem$chemical==chemical,colnames(chem)%in%Names_fix],
                  fPC[fPC$species==species,colnames(fPC)%in%Names_fix],
                  fBW[fBW$species==species,colnames(fBW)%in%substr(Names_var_not[grep('fBW',Names_var_not)],
                                                                   start=5,stop=nchar(Names_var_not[grep('fBW',Names_var_not)]))],
                  fCO[fCO$species==species,colnames(fCO)%in%substr(Names_var_not[grep('fCO',Names_var_not)],
                                                                   start=5,stop=nchar(Names_var_not[grep('fCO',Names_var_not)]))],
                  rates[rates$species==species,colnames(rates)%in%Names_var_not])
  colnames(fix_in) <- Names_fix

  #create data frames with random samples
  X1 <- matrix(NA, nrow = n_sim, ncol = NP_var)
  colnames(X1) <- Names_var
  X1 <- as.data.frame(X1)

  X2 <- matrix(NA, nrow = n_sim, ncol = NP_var)
  colnames(X2) <- colnames(X1)
  X2 <- as.data.frame(X2)

  for(i in 1:NP_var){
    X1[,i] <- runif(n_sim, min = Lower[,i], max = Upper[,i])
    X2[,i] <- runif(n_sim, min = Lower[,i], max = Upper[,i])
  }

  #Sobol design
  sa <- soboljansen(model = NULL, X1, X2, nboot = n_boot, conf = 0.95)
  SARes <- sa$X



} else if (A_type=="SA") {
#Sensitivity analysis with fixed chem parameters and varying physiology
  #initial list with names of all varying parameters
  Names_var <- c(colnames(TK[3:8]),
                 colnames(chem[2:5]))
```

```
#initial lower and upper limits for uniform distributions
Lower <- as.data.frame(cbind(0,0,0,NA,NA,NA,10,0.001,0.00001,0.01))
Upper <- as.data.frame(cbind(1,1,1,NA,NA,NA,1000,1000,10000000000000,100000))
colnames(Lower) = colnames(Upper) = Names_var

Names_var_not <- colnames(Lower[which(is.na(Lower))])

Lower <- Lower[!(colnames(Lower)%in%Names_var_not)] #exclude all compartments for which median = 0 or NA
Upper <- Upper[!(colnames(Upper)%in%Names_var_not)] #exclude all compartments for which median = 0 or NA

Names_var <- colnames(Lower)
NP_var <- length(Names_var) #number of varying parameters

#list with names of all fixed parameters (including 'varying parameters' that are 0 or NA)
Names_fix <- c("BW",
               paste("fBW",colnames(fBW[2+3*c(1:19)]),sep="_"),
               "CO",
               paste("fCO",colnames(fCO[2+3*c(1:19)]),sep="_"),
               colnames(rates[2+3*c(0:4)]),
               colnames(fPC[2:57]),
               "nl","pl","pr","w",
               Names_var_not)
NP_fix <- length(Names_fix) #number of fixed parameters

fix_in <- cbind(fBW[fBW$species==species,"BW"],
                fBW[fBW$species==species,colnames(fBW)%in%substr(Names_fix[grep('fBW',Names_fix)],
                                                                 start=5,stop=nchar(Names_fix[grep('fBW',Names_fix)]))],
                fCO[fCO$species==species,"CO"],
                fCO[fCO$species==species,colnames(fCO)%in%substr(Names_fix[grep('fCO',Names_fix)],
                                                                 start=5,stop=nchar(Names_fix[grep('fCO',Names_fix)]))],
                rates[rates$species==species,colnames(rates)%in%Names_fix],
                fPC[fPC$species==species,colnames(fPC)%in%Names_fix],
                data.frame(nl=1,pl=1,pr=1,w=1),
                TK[TK$species==species&TK$chemical==chemical,colnames(TK)%in%Names_var_not],
                chem[chem$chemical==chemical,colnames(chem)%in%Names_var_not])
colnames(fix_in) <- Names_fix

#Change upper limit for clearance depending on physiology of species of interest
  #renal clearance = blood flow to kidneys
  Upper[,"Cl_renal"] <- fix_in$fCO_kidney * fix_in$CO / fix_in$BW
```

```
    #hepatic clearance = blood flow to liver (incl portal artery)
    Upper[,"Cl_hepatic"] <- (fix_in$fCO_liver+fix_in$fCO_intestine)*fix_in$CO/fix_in$BW

  #create data frames with random samples
  X1 <- matrix(NA, nrow = n_sim, ncol = NP_var)
  colnames(X1) <- Names_var
  X1 <- as.data.frame(X1)

  X2 <- matrix(NA, nrow = n_sim, ncol = NP_var)
  colnames(X2) <- colnames(X1)
  X2 <- as.data.frame(X2)

  for(i in 1:NP_var){
    X1[,i] <- runif(n_sim, min = Lower[,i], max = Upper[,i])
    X2[,i] <- runif(n_sim, min = Lower[,i], max = Upper[,i])
  }

  #Sobol design
  sa <- soboljansen(model = NULL, X1, X2, nboot = n_boot, conf = 0.95)
  SARes <- sa$X

} else if (A_type=="VA") {
  #variability analysis with fixed chemical and TK parameters
  Names_var <- c("BW",
                 paste("fBW",colnames(fBW[2+3*c(1:19)]),sep="_"),
                 "CO",
                 paste("fCO",colnames(fCO[2+3*c(1:19)]),sep="_"),
                 colnames(rates[2+3*c(0:4)]))

  #initial list with mean + sd values of all varying parameters
  Means <- cbind(fBW[fBW$species==species,2+3*c(0:19)],
                 fCO[fCO$species==species,2+3*c(0:19)],
                 rates[rates$species==species,2+3*c(0:4)])
  SDs <- cbind(fBW[fBW$species==species,3+3*c(0:19)],
               fCO[fCO$species==species,3+3*c(0:19)],
               rates[rates$species==species,3+3*c(0:4)])
  Distributions <- cbind(fBW[fBW$species==species,4+3*c(0:19)],
                         fCO[fCO$species==species,4+3*c(0:19)],
                         rates[rates$species==species,4+3*c(0:4)])
  colnames(Means) = colnames(SDs) = colnames(Distributions) = Names_var
```

```
Names_var_not <- colnames(SDs[which(is.na(SDs))])

Means <- Means[!(colnames(Means)%in%Names_var_not)] #exclude all parameters without SD
SDs <- SDs[!(colnames(SDs)%in%Names_var_not)] #exclude all parameters without SD
Distributions <- Distributions[!(colnames(Distributions)%in%Names_var_not)] #exclude all parameters without SD

Names_var <- colnames(SDs)
NP_var <- length(Names_var) #number of varying parameters

#list with names of all fixed parameters (including 'varying parameters' that are 0 or NA)
Names_fix <- c(colnames(fPC[2:57]),
               "nl","pl","pr","w",
               colnames(TK[3:8]),
               colnames(chem[2:5]),
               Names_var_not)
NP_fix <- length(Names_fix) #number of fixed parameters

fix_in <- cbind(fPC[fPC$species==species,colnames(fPC)%in%Names_fix],
                data.frame(nl=1,pl=1,pr=1,w=1),
                TK[TK$species==species&TK$chemical==chemical,colnames(TK)%in%Names_fix],
                chem[chem$chemical==chemical,colnames(chem)%in%Names_fix],
                fBW[fBW$species==species,colnames(fBW)%in%substr(Names_fix[grep('fBW',Names_fix)],
                                                                 start=5,stop=nchar(Names_fix[grep('fBW',Names_fix)]))],
                fCO[fCO$species==species,colnames(fCO)%in%substr(Names_fix[grep('fCO',Names_fix)],
                                                                 start=5,stop=nchar(Names_fix[grep('fCO',Names_fix)]))],
                rates[rates$species==species,colnames(rates)%in%Names_fix])
colnames(fix_in) <- Names_fix

#create data frames with random samples
X1 <- matrix(NA, nrow = n_sim, ncol = NP_var)
colnames(X1) <- Names_var
X1 <- as.data.frame(X1)
SARes <- X1

for(i in 1:NP_var){
  if (Distributions[i] == "N") {
    SARes[,i] <- rnorm(n_sim, mean = Means[,i], sd = SDs[,i])
  } else if (Distributions[i] == "B") {
    alpha <- ((1 - Means[,i]) / SDs[,i]^2 - 1 / Means[,i]) * Means[,i] ^ 2
    beta <- alpha * (1 / Means[,i] - 1)
```

```
      SARes[,i] <- rbeta(n_sim, shape1 = alpha, shape2 = beta)
    } else if (Distributions[i] == "LN") {
      CV <- SDs[,i]/Means[,i]
      mlog <- log(Means[,i]/sqrt(1+CV^2)) #mean of log values
      slog <- sqrt(log(1+CV^2)) #sd of log values
      SARes [,i] <- rlnorm(n_sim, meanlog = mlog, sdlog = slog)
    }
  }
}

#=============================================================================================
# Model run for probabilistic analysis (to be done on separate server) ----
  for (k in 1:(nrow(SARes)/1000)) {
    var_in_temp <- SARes[c((1+1000*(k-1)):(k*1000)),]
    par_in <- cbind(var_in_temp, fix_in)
    #adjust clearance rates of hypothetical chemicals based on values drawn for physiology
    if (chem_fix & (chemical=="chem1"|chemical=="chem2"|chemical=="chem3")) {
      par_in$Cl_renal <- par_in$Cl_renal*par_in$fCO_kidney*par_in$CO / par_in$BW
      par_in$Cl_hepatic <- par_in$Cl_hepatic*(par_in$fCO_intestine+par_in$fCO_liver)*par_in$CO / par_in$BW
    }
    write.csv(par_in,file=paste("par_in_chik_oral8.6", k, ".csv",sep=""),row.names = FALSE)
  }

#=============================================================================
#Model application ------

  #sub_in <- 1
  source('singchem_dmdt_Sary.R')
  #par_in <- read.csv(paste("par_in_chik_oral8.61.csv",sep=""))
  SimRes <- matrix(NA, nrow = nrow(par_in), ncol = n_out*length(t_A))
  colnames(SimRes) <- c(paste("blood_t",t_A,sep=""),paste("liver_t",t_A,sep=""),paste("kidney_t",t_A,sep=""),
                        paste("brain_t",t_A,sep=""),paste("heart_t",t_A,sep=""),paste("lung_t",t_A,sep=""),paste("muscle_t",t_A,sep=""))

  for (j in 1:nrow(par_in)) {
    print(paste0("Running loop: ", j))
    print(paste("Current time: ", Sys.time()))

    SimRes[j,] <- multi_tool(
      par_in = par_in[j,], #input data frame
      species = species, regime = regime, route = route, E_dose = E_dose, E_start = E_start, E_end = E_end, E_int = E_int,
```

```
                                #exposure scenario
      n_out = n_out, t_start = t_start, t_end = t_end, t_A = t_A, chem_fix = chem_fix)
  }

write.csv(SimRes,paste("goat_chloramphenicol_tryout.csv",sep=""),row.names = FALSE)

#=============================================================================
#Plot Concentrations vs time
ivermectin_lung.data <- read.csv(file="ivermectin_lung.csv")

p1 <- ggplot(data = ivermectin_lung.data, aes(x = Hours, y = Value, group = Compartment)) +
  geom_point(aes(color = Compartment)) +
  geom_line(aes(color = Compartment))

p1 + labs(title = "Ivermectin in Lungs", x = "Time after Exposure (hours)", y = "Concentration (\u03bcg/mL)")

#=============================================================
#Plot Log measured vs predicted concentrations
ivermectin_lung.data <- read.csv(file="ivermectin_lung2.csv")

p2 <- ggplot(data = ivermectin_lung.data, aes(x = Measurement, y = Model)) +
  geom_point() +
  geom_abline(intercept= 0, slope=1, col="red") +
  geom_abline(intercept=log10(10), slope=1, col="darkgrey") +
  geom_abline(intercept =-log10(10), slope = 1, col="darkgrey")

p2 + scale_x_log10(limits = c(1e-6,1e-1)) +
  scale_y_log10(limits = c(1e-6,1e-1)) +
  labs(title = "Ivermectin in Lungs", x = "Measured concentration (\u03bcg/mL))", y = "Predicted concentration (\u03bcg/mL)")

#=============================================================
#Plot log concentrations vs time
ivermectin_lung.data <- read.csv(file="ivermectin_lung.csv")

p3 <- ggplot(data = ivermectin_lung.data, aes(x = Hours, y = Value, group = Compartment)) +
  geom_point(aes(color = Compartment)) +
  geom_line(aes(color = Compartment))

p3 + scale_y_log10() +
  labs(title = "Ivermectin in Lungs", x = "Time after Exposure (hours)", y = "Concentration (\u03bcg/mL)")
```

```
dMdt <- function(i, M, C, h, physnames,
                 Qin, Qout, CO, PC, OW,
                 E_bolus, E_cont, E_iv, kgastric,
                 Qbolus, Qingest, Qiv, Qexhale,
                 kabs, Vmax, Km, Cl, fbile, fbact,
                 Qegg, Qmilk) {
  #input via food
  dMfood <- E_bolus[i] * Qbolus + E_cont[i] * Qingest
  #input via iv
  dMiv <- E_iv[i] * Qiv
  #absorption over intestinal wall
  dMabs <- M[physnames=="lumen"] * kabs
  #delivery via arterial blood
  dMart <- Qin * C[physnames=="art"]
  dMart[physnames=="art"] <- -sum(dMart)
  #delivery to venous blood and passage through portal vein
  dMven <- Qout * (C / PC)
  dMart[physnames=="liver"] <- dMart[physnames=="liver"] - dMven[physnames=="intestine"]
  dMven[physnames=="liver"] <- dMven[physnames=="liver"] + Qout[physnames=="intestine"] * (C[physnames=="liver"] / PC[physnames=="liver"])
  dMven[physnames=="ven"] <- -sum(dMven[physnames!="intestine"])
  #metabolism an enterohepatic circulation and retransformation
  dMmet <- ifelse(!is.na(Vmax)&!is.na(Km),(Vmax*(C/PC))/(Km+(C/PC))*OW,0)
  dMmet[physnames=="liver"] <- ifelse(!is.na(Cl[physnames=="liver"]),Cl[physnames=="liver"]*C[physnames=="liver"])
  dMmet[physnames=="lumen"] <- -dMmet[physnames=="liver"] * fbile * fbact
  dMmet[physnames=="metab"] <- -dMmet[physnames=="liver"] - dMmet[physnames=="lumen"]
  #transport over lung and exhalation
  dMexh <- -CO * C
  dMexh[physnames!="ven"] <- 0
  dMexh[physnames=="art"] <- -dMexh[physnames=="ven"] * (CO / (CO + Qexhale * PC[physnames=="air"]))
  dMexh[physnames=="air"] <- -dMexh[physnames=="ven"] * ((Qexhale * PC[physnames=="air"])/(CO + Qexhale * PC[physnames=="air"]))
  #excretion to urine, milk, eggs, feces
  dMexc <- M[physnames=="lumen"] * kgastric
  dMexc[physnames=="kidney"] <- C[physnames=="kidney"] * Cl[physnames=="kidney"]
  dMexc[physnames=="reprod"] <- C[physnames=="reprod"] * Qegg[physnames=="reprod"]
  dMexc[physnames=="mamgland"] <- C[physnames=="mamgland"] * Qmilk[physnames=="mamgland"]
  dMexc[physnames=="urine"] <- -dMexc[physnames=="kidney"]
  dMexc[physnames=="egg"] <- -dMexc[physnames=="reprod"]
  dMexc[physnames=="milk"] <- -dMexc[physnames=="mamgland"]

  dMdt <- dMfood + dMiv + (dMabs + dMart + dMven + dMmet + dMexh + dMexc) * (h / 60)
```

```
  M <- M + dMdt
  C <- ifelse(OW==0,0,M/OW)

  return(list(M=M,C=C))
}

#Function to run model
multi_tool <- function(par_in, species, regime, route, E_dose, E_start, E_end, E_int, n_out, t_start, t_end, t_A, chem_fix) {

  #Physicochemical properties ----
  MW <- par_in$MW
  Kow <- par_in$Kow #Kow
  S <- (0.001*par_in$S) / MW #solubility
  Temp <- 298        #Temperature 298 K = 25 degC
  R <- 8.314         #Gas constant (J/mol/K)
  Pv <- par_in$Pv #vapor pressure

  #General physiology ----
  BW <- par_in$BW              #bodyweight (kg)
  CO <- par_in$CO          #cardiac output (L/min)

  if (species=="chicken") {
    Qexhale <- ((284 * (BW^0.77))/1000)    #Ventilation avian (L/min)
  } else {
    Qexhale <- (0.499 * (BW^0.81))         #Ventilation mammalian (L/min)
  }

  #one matrix per relevant phys parameter (in right order)
  comp <- colnames(par_in[grep('fBW',colnames(par_in))])
  comp <- comp[order(comp)]
  physnames <- c(substr(comp,start=5,stop=nchar(comp)),"ven","art","lumen","milk","egg","urine","air","feces","metab","feed","iv")

  #Organ weights
  fBW <- c(t(par_in[comp]),rep(0,11))
  fBW[physnames=="ven"] <-  2/3 * fBW[physnames=="blood"]
  fBW[physnames=="art"] <-  1/3 * fBW[physnames=="blood"]
  fBW <- fBW[physnames!="blood"]
  OW <- BW*fBW/sum(fBW) #organ volums (L), based on normalized weight fractions and overall assumed density of 1 L/kg
```

```
#Blood flows Q
comp <- gsub('fBW','fCO',comp)
fCO <- c(t(par_in[comp]),rep(0,11))
fCO <- (fCO[physnames!="blood"])
Qin <- fCO*CO/sum(fCO) #blood flows (L/min), normalized to CO
Qout <- -Qin

#Tissue-blood partitioning
comp <- c(colnames(par_in[grep('_nl',colnames(par_in))]),colnames(par_in[grep('_pl',colnames(par_in))]),
          colnames(par_in[grep('_pr',colnames(par_in))]),colnames(par_in[grep('_w',colnames(par_in))]))
comp <- comp[order(comp)]

PCcomp <- comp[c(-grep('exp_',comp),-grep('int_',comp))] #all tissue composition -names
fPC_old <- c(t(par_in[PCcomp])) #'old fractions'
fPC_new <- fPC_old*c(par_in$nl,par_in$pl,par_in$pr,par_in$w) #new fractions

  #normalisation to mean sum
  sumold <- rep(tapply(fPC_old,rep(seq(length(fPC_old)/4),each=4),sum),each=4)
  sumnew <- rep(tapply(fPC_new,rep(seq(length(fPC_old)/4),each=4),sum),each=4)
  fPC_new <- fPC_new*(sumold/sumnew)

PCexps <- comp[grep('exp_',comp)]
fPC_exp <- c(t(par_in[PCexps]))    #all QSAR exponents
PCints <- comp[grep('int_',comp)]
fPC_int <- c(t(par_in[PCints]))    #all QSAR intercepts

tissnames <- c(substr(PCcomp[grep('_nl',PCcomp)],start=1,stop=nchar(PCcomp[grep('_nl',PCcomp)])-3))
PC1 <- fPC_int*fPC_new*Kow^fPC_exp
PC1 <- tapply(fPC_int*fPC_new*Kow^fPC_exp,rep(seq(length(PC1)/4),each=4),sum) #partitioning coefficients tissue-water
PC <- rep(PC1[tissnames=="blood"],length(physnames))
PC[match(tissnames,physnames)] <- PC1
PC[physnames=="air"] <- (Pv/S)/(R*Temp)
PC[physnames=="stomach"|physnames=="abomasum"|physnames=="omasum"|physnames=="rumen"|
     physnames=="reticulum"|physnames=="gizzard"|physnames=="crop"] <- PC[physnames=="intestine"]
PC[is.na(PC)] <- PC[physnames=="blood"]
PC <- PC/PC[physnames=="blood"]
PC <- PC[physnames!="blood"]

#Rates and flows (not chemical-dependent)
physnames <- physnames[physnames!="blood"]
```

```
Qingest <- rep(0,length(physnames))
Qiv <- rep(0,length(physnames))
Qbolus <- rep(0,length(physnames))
kgastric <- rep(0,length(physnames))
Qmilk <- rep(0,length(physnames))
Qegg <- rep(0,length(physnames))
fbile <- par_in$fbile #fraction of metabolites reentering lumen with bile (-)

Qingest[physnames=="lumen"] <- par_in$Qingest / (24*60) #ingestion rate kgfeed/min
Qingest[physnames=="feed"] <- -par_in$Qingest / (24*60)
Qiv[physnames=="ven"] <- 1
Qiv[physnames=="iv"] <- -1
Qbolus[physnames=="lumen"] <- 1
Qbolus[physnames=="feed"] <- -1
kgastric[physnames=="feces"] <- par_in$kgastric
kgastric[physnames=="lumen"] <- -par_in$kgastric#gastric emptying rate constant (1/min)
Qmilk[physnames=="mamgland"&Qin!=0] <- -par_in$Qmilk #milk production rate (L/min)
Qegg[physnames=="reprod"&Qin!=0] <- -par_in$Qegg #egg production rate (L/min)

#TK parameters
kabs <- rep(0,length(physnames))
Vmax <- rep(NA,length(physnames))
Km <- rep(NA,length(physnames))
Cl <- rep(0,length(physnames))

fbact <- par_in$fbact
kabs[physnames=="intestine"] <- par_in$kabs
kabs[physnames=="lumen"] <- -par_in$kabs
Vmax[physnames=="liver"] <- -par_in$Vmax_tot
Km[physnames=="liver"] <- par_in$Km_tot
#Cl[physnames=="liver"] <- -par_in$Cl_hepatic * BW * par_in$inhibit
Cl[physnames=="liver"] <- -par_in$Cl_hepatic * BW
Cl[physnames=="kidney"] <- -par_in$Cl_renal * BW


#Time vector for exposure -----
h <- 3 #stepsize in seconds
t <- seq(3600*t_start,3600*t_end,by=h)       #vector with timepoints (seconds)
#E_dose <- par_in$E_dose                      #only becuase of varibilaity in bioavailability, otherwise
                                              #E_dose needs to be desrcibed in multi_tool
```

```
  E_iv <- rep(0,times=length(t))
  E_bolus <- rep(0,times=length(t))
  E_cont <- rep(0,times=length(t))

  if (route=="oral" & regime == "bolus") {
    E_bolus[t>=E_start*3600 & t<3600*E_end & t%%(3600*E_int)==0] <- (E_dose/MW)*BW
  } else if (route=="oral" & regime == "continuous") {
    #E_cont[t>=E_start*3600 & t<3600*E_end] <- E_dose/MW
    E_cont[t>=E_start*3600 & t<3600*E_end] <- ((E_dose/MW)/par_in$Qingest)*BW #mmol/kgfeed
  } else {
    E_iv[t==E_start*3600] <- (E_dose/MW)*BW
  }

  M <- rep(0,length(physnames)) #mass per compartment (mmol)
  C <- rep(0,length(physnames)) #concentration per compartment (mmol/L)

#Create output sheet ----
  if (chem_fix) {
    results <- matrix(NA,nrow=1,ncol=n_out*length(t_A))
    colnames(results) <- c(paste("blood_t",t_A,sep=""),paste("liver_t",t_A,sep=""),paste("kidney_t",t_A,sep=""),
                           paste("brain_t",t_A,sep=""),paste("heart_t",t_A,sep=""),paste("lung_t",t_A,sep=""),paste("muscle_t",t_A,sep=""))
    #colnames(results) <- c(paste("blood_t",t_A,sep=""))
  } else {
    results <- matrix(0,nrow=1,ncol=3)
    colnames(results) <- c("Cmax","tmax","AUC_24h")
  }

#Model simulation ----

  for (i in 1:length(t)) {
    output <- dMdt(i=i, M=M, C=C, h=h, physnames=physnames, Qin=Qin, Qout=Qout, CO=CO,
                   PC=PC, OW=OW, E_bolus=E_bolus, E_cont=E_cont, E_iv=E_iv, kgastric=kgastric,
                   Qbolus=Qbolus, Qingest=Qingest, Qiv=Qiv, Qexhale=Qexhale, kabs=kabs, Vmax=Vmax,
                   Km=Km, Cl=Cl, fbile=fbile, fbact=fbact, Qegg=Qegg, Qmilk=Qmilk)

    M <- output$M
    C <- output$C

#Write to results for t_A
    if (chem_fix & any(t[i]==round(t_A*3600))) {
```

```
    results[,paste("blood_t",t[i]/3600,sep="")] <- C[physnames=="ven"] * MW
    #results[,paste("fat_t",t[i]/3600,sep="")] <- C[physnames=="adipose"]* MW
    #results[,paste("mamgland_t",t[i]/3600,sep="")] <- C[physnames=="mamgland"]* MW
    results[,paste("liver_t",t[i]/3600,sep="")] <- C[physnames=="liver"] * MW
    results[,paste("kidney_t",t[i]/3600,sep="")] <- C[physnames=="kidney"] * MW
    results[,paste("muscle_t",t[i]/3600,sep="")] <- C[physnames=="muscle"] * MW
    results[,paste("heart_t",t[i]/3600,sep="")] <- C[physnames=="heart"] * MW
    results[,paste("brain_t",t[i]/3600,sep="")] <- C[physnames=="brain"] * MW
    #results[,paste("carcass_t",t[i]/3600,sep="")] <- C[physnames=="carcass"] * MW
    #results[,paste("abomasum_t",t[i]/3600,sep="")] <- C[physnames=="abomasum"] * MW
    #results[,paste("intestine_t",t[i]/3600,sep="")] <- C[physnames=="intestine"] * MW
    results[,paste("lung_t",t[i]/3600,sep="")] <- C[physnames=="lung"] * MW
    #results[,paste("reprod_t",t[i]/3600,sep="")] <- C[physnames=="reprod"] * MW
    #results[,paste("egg_t",t[i]/3600,sep="")] <- M[physnames=="egg"] * MW   #mg
    #results[,paste("milk_t",t[i]/3600,sep="")] <- M[physnames=="milk"] * MW   #mg

  } else if (!chem_fix) {
    results[,"tmax"] <- ifelse(C[physnames=="ven"]>results[,"Cmax"],t[i]/3600,results[,"tmax"])
    results[,"Cmax"] <- ifelse(C[physnames=="ven"]>results[,"Cmax"],C[physnames=="ven"],results[,"Cmax"])
    results[,"AUC_24h"] <- results[,"AUC_24h"] + C[physnames=="ven"]
  }
}

  return(results)
}
```

Appendix B

Results

Table B.1: Results of the measured concentrations by Lespine et al. (2005) and the model predicted concentrations for Ivermectin. ND = non-detected.

(a) Ivermectin concentrations in plasma.

Hours after exposure	**Measured value (μg/mL)**	**Predicted value (μg/mL)**
24		0.026
48	0.0060	0.0047
120		$2.78*10^{-5}$
168	0.0004	$9.02*10^{-7}$
240		$5.28*10^{-9}$
336		$5.85*10^{-12}$
408	ND	$3.26*10^{-14}$

(b) Ivermectin concentrations in lungs.

Hours after exposure	**Measured value (μg/mL)**	**Predicted value (μg/mL)**
24		0.052
48	0.0181	0.0098
120		$5.71*10^{-5}$
168	0.001	$1.85*10^{-6}$
240		$1.09*10^{-8}$
336		$1.41*10^{-11}$
408	ND	$6.69*10^{-14}$

(c) Ivermectin concentrations in abomasal mucosa.

Hours after exposure	**Measured value (μg/mL)**	**Predicted value (μg/mL)**
24		0.0305
48	0.0174	0.0055
120		$3.24*10^{-5}$
168	0.00078	$1.05*10^{-6}$
240		$6.15*10^{-9}$
336		$6.48*10^{-12}$
408	ND	$3.79*10^{-14}$

(d) Ivermectin concentrations in intestinal mucosa.

Hours after exposure	**Measured value (μg/mL)**	**Predicted value (μg/mL)**
24		0.0307
48	0.0236	0.0055
120		$3.25*10^{-5}$
168	0.0014	$1.05*10^{-6}$
240		$6.17*10^{-9}$
336		$6.50*10^{-12}$
408	ND	$3.80*10^{-14}$

(e) Ivermectin concentrations in liver.

Hours after exposure	**Measured value (μg/mL)**	**Predicted value (μg/mL)**
24		0.053
48	0.042	0.0096
120		$5.62*10^{-5}$
168	0.0015	$1.82*10^{-6}$
240		$1.08*10^{-8}$
336		$1.13*10^{-11}$
408	ND	$6.58*10^{-14}$

(f) Ivermectin concentrations in fat.

Hours after exposure	**Measured value (μg/mL)**	**Predicted value (μg/mL)**
24		0.024
48	0.062	0.0044
120		$2.57*10^{-5}$
168	0.0048	$8.33*10^{-7}$
240		$4.88*10^{-9}$
336		$5.14*10^{-12}$
408	0.00034	$3.01*10^{-14}$

Table B.2: Results of the measured concentrations by Etuk & Onyeyili (2005) and the model predicted concentrations for Chloramphenicol.

(a) Chloramphenicol concentrations in brain.

Hours after exposure	**Measured value (μg/mL)**	**Predicted value (μg/mL)**
0.08	0.1	2.02
0.25	0.36	4.54
0.5	0.63	7.73
1	0.41	12.8
3	0.32	22.0
6	0.28	24.0
12	0.18	21.9
24	0.10	17.1
48	0.00	10.5
120		2.45
240		0.276

(b) Chloramphenicol concentrations in heart.

Hours after exposure	**Measured value (μg/mL)**	**Predicted value (μg/mL)**
0.08	34.6	3.62
0.25	18.0	7.98
0.5	8.94	13.2
1	6.82	20.6
3	4.03	30.6
6	3.22	30.6
12	1.04	27.1
24	0.46	21.3
48	0.10	13.1
120		3.03
240		0.266

(c) Chloramphenicol concentrations in kidney.

Hours after exposure	**Measured value (μg/mL)**	**Predicted value (μg/mL)**
0.08	53.0	0.717
0.25	26.2	0.677
0.5	13.2	0.665
1	10.2	0.648
3	7.03	0.602
6	5.16	0.560
12	4.33	0.495
24	4.02	0.388
48	3.61	0.239
120	0.83	0.055
240	0.1	0.005

(d) Chloramphenicol concentrations in liver.

Hours after exposure	**Measured value (μg/mL)**	**Predicted value (μg/mL)**
0.08	69.0	0.382
0.25	35.1	1.65
0.5	18.3	4.32
1	14.3	10.5
3	11.0	26.5
6	8.42	30.8
12	7.06	28.2
24	6.32	22.1
48	2.09	13.6
120	0.38	3.15
240		0.276

(e) Chloramphenicol concentrations in lungs.

Hours after exposure	**Measured value (μg/mL)**	**Predicted value (μg/mL)**
0.08	39.0	2.06
0.25	19.3	4.64
0.5	8.78	7.88
1	7.01	12.9
3	5.21	22.1
6	3.04	24.0
12	1.33	21.8
24	0.98	17.1
48	0.14	2.43
120	0.14	10.5
240		0.21

(f) Chloramphenicol concentrations in muscle.

Hours after exposure	**Measured value (μg/mL)**	**Predicted value (μg/mL)**
0.08	0.93	31.6
0.25	1.26	28.4
0.5	2.98	28.4
1	4.62	27.1
3	3.98	25.2
6	3.90	23.4
12	3.64	20.7
24	2.98	16.2
48	1.07	9.97
120	0.54	2.31
240	0.12	0.20

Table B.3: Results of the measured concentrations by Fernandez-Varon et al. (2006) and the model predicted concentrations for Moxifloxacin.

(a) Moxifloxacin concentrations in plasma.

Hours after exposure	**Measured value (μg/mL**	**Predicted value (μg/mL)**
0.08	8.07	6.42
0.17	6.03	6.19
0.25	6.03	6.11
0.5	4.86	5.99
0.75	3.86	5.90
1	3.36	5.81
1.5	2.51	5.66
2	1.74	5.53
4	0.651	5.09
6	0.259	4.72
8	0.071	4.39
10	0.035	4.08
12	0.022	3.79
24		2.44
32		1.82
48		1.01
72		0.42

(b) Moxifloxacin concentrations in milk.

Hours after exposure	**Measured value (μg/mL)**	**Predicted value (μg/mL)**
2	3.59	22.2
4	2.27	21.0
6	0.919	18.7
8	0.421	16.8
10	0.182	15.0
24	0.030	9.92
32	0.015	5.34
48		2.83
72		0.98